

## Chapter 9

# Seiches and Harbor Oscillations

Alexander B. Rabinovich

*P.P. Shirshov Institute of Oceanology, Russian Academy of Sciences  
36 Nakhimovsky Prosp., Moscow, 117997 Russia*

*Department of Fisheries and Oceans, Institute of Ocean Sciences  
9860 West Saanich Road, Sidney, BC, Canada V8L 4B2  
a.b.rabinovich@gmail.com  
alexander.rabinovich@dfo-mpo.gc.ca*

This chapter presents an overview of seiches and harbor oscillations. *Seiches* are long-period standing oscillations in an enclosed basin or in a locally isolated part of a basin. They have physical characteristics similar to the vibrations of a guitar string or an elastic membrane. The resonant (eigen) periods of seiches are determined by basin geometry and depth and in natural basins may range from tens of seconds to several hours. The set of seiche eigen frequencies (periods) and associated modal structures are a fundamental property of a particular basin and are independent of the external forcing mechanism. *Harbor oscillations* (coastal seiches) are a specific type of seiche motion that occur in partially enclosed basins (bays, fjords, inlets, and harbors) that are connected through one or more openings to the sea. In contrast to seiches, which are generated by direct external forcing (e.g., atmospheric pressure, wind, and seismic activity), harbor oscillations are mainly generated by long waves entering through the open boundary (harbor entrance) from the open sea. Energy losses of seiches in enclosed basins are mostly due to dissipative processes, while the decay of harbor oscillations is primarily due to radiation through the mouth of the harbor. An important property of harbor oscillations is the *Helmholtz mode* (pumping mode), similar to the fundamental tone of an acoustic resonator. This mode is absent in a closed basin.

Harbor oscillations can produce damaging *surging* (or *range action*) in some ports and harbors yawing and swaying of ships at berth in a harbor. A property of oscillations in harbors is that even relatively small vertical motions (sea level oscillations) can be accompanied by large horizontal motions (harbor currents), resulting in increased risk of damage of moored ships, breaking mooring lines as well as affecting various harbor procedures. Tsunamis constitute another important problem: catastrophic destruction may occur when the frequencies of arriving tsunami waves match the resonant frequencies of the harbor or bay.

Seiches, as natural resonant oscillations, are generated by a wide variety of mechanisms, including tsunamis, seismic ground waves, internal ocean waves, and

jet-like currents. However, the two most common factors initiating seiches are atmospheric processes and nonlinear interaction of wind waves or swell. At certain places in the World Ocean, waves due to atmospheric forcing (atmospheric gravity waves, pressure jumps, frontal passages, squalls) can be responsible for significant, even devastating harbor oscillations, known as *meteorological tsunamis*. They have the same temporal and spatial scales as typical tsunami waves and can affect coasts in a similar damaging way.

## 9.1. Introduction

*Seiches* are long-period standing oscillations in an enclosed basin or in a locally isolated part of a basin (in the Japanese literature they are commonly known as “*secondary oscillations (undulations) of tides*”).<sup>30,56,59</sup> The term “seiches” apparently originated from the Latin word *siccus* which means dry or exposed (from the exposure of the littoral zone at the down-swing).<sup>31,95</sup> Free-surface oscillations, known as *seiches* or *seiching* in lakes and harbors or as *sloshing* in coffee cups, bathtubs, and storage tanks, have been observed since very early times; a vivid description of seiching in Lake Constance, Switzerland, was given in 1549, and the first instrumental record of seiches obtained in 1730 in Lake Geneva.<sup>46,95</sup> Korgen<sup>34</sup> describes seiches as “*the rhythmic, rocking motions that water bodies undergo after they have been disturbed and then sway back-and-forth as gravity and friction gradually restore them to their original, undisturbed conditions.*” These oscillations occur at the *natural* resonant periods of the basin (so-called “*eigen periods*”) and physically are similar to vibrations of a guitar string and an elastic membrane. The resonant (*eigen*) periods of seiches are determined by the basin geometry and depth<sup>94,95</sup> and in natural basins may be from a few tens of seconds to several hours. The oscillations are known as *natural* (or *eigen*) *modes*. The mode with the lowest frequency (and thus, the longest period) is referred to as the *fundamental mode*.<sup>41</sup>

The set of seiche eigen frequencies (periods) and associated modal structures are a fundamental property of a particular basin and are independent of the external mechanism forcing the oscillations. In contrast, the amplitudes of the generated seiches strongly depend on the energy source that generates them, and can therefore have pronounced variability.<sup>31</sup> Resonance occurs when the dominant frequencies of the external forcing match the eigen frequencies of the basin.

*Harbor oscillations* (*coastal seiches* according to Ref. 19 are a specific type of seiche motion that occur in partially enclosed basins (gulfs, bays, fjords, inlets, ports, and harbors) that are connected through one or more openings to the sea.<sup>41,94</sup> Harbor oscillations differ from seiches in closed water bodies (for example, in lakes) in three principal ways<sup>68</sup>:

- (1) In contrast to seiches generated by direct external forcing (e.g., atmospheric pressure, wind, and seismic activity), harbor oscillations are mainly generated by long waves entering through the open boundary (harbor entrance) from the open sea.

- (2) Energy losses of seiches in closed basins are mostly associated with dissipation, while the decay of harbor oscillations is mainly due to radiation through the mouth of the harbor.
- (3) Harbor oscillations have a specific fundamental mode, the *Helmholtz mode*, similar to the fundamental tone of an acoustic resonator.<sup>54</sup> This modes is absent in closed basins.

Because harbor oscillations can produce damaging *surging* (or *range action*) — yaw and swaying of ships at berth in a harbor — this problem has been extensively examined in the scientific and engineering literature.<sup>4,11,12,36,41,46,47,62,67,68,70,78,79,94,95</sup> One of the essential properties of oscillations in harbors is that even relatively small vertical motions (sea level oscillations) can be accompanied by large horizontal water motions (harbor currents); when the period of these motions coincides with the natural period of sway, or yaw of a moored ship, further resonance occurs, which can result in considerable motion and possible damage of a moored ship.<sup>82,94</sup> Harbor oscillations can also break mooring lines, cause costly delays in loading and unloading operations at port facilities, and seriously affect various harbor procedures.<sup>79,80</sup>

Tsunamis constitute another important problem that have greatly stimulated investigations of harbor oscillations. Professor Omori (Japan) was likely the first to notice in 1902 that the dominant periods of observed tsunami waves are normally identical to those caused by ordinary long waves in the same coastal basin (see Ref. 30). His explanation was that the bay or portion of the sea oscillates like a fluid pendulum with its own period, i.e., the arriving tsunami waves generate similar seiches as those generated by atmospheric processes and other types of external forcing (see also Ref. 30). Numerous papers on the spectral analysis of tsunami records for various regions of the world ocean have confirmed this conclusion.<sup>13,48,69,74,75,84,90</sup> Catastrophic destruction may occur when the frequencies of arriving tsunami waves match the resonant frequencies of the harbor or bay. One of the best examples of strong tsunami amplification due is the resonant response of Port Alberni (located at the head of long Alberni Inlet on the Pacific coast of Vancouver Island, Canada) to the 1964 Alaska tsunami.<sup>28,54</sup>

## 9.2. Hydrodynamic Theory

The basic theory of seiche oscillations is similar to the theory of free and forced oscillations of mechanical, electrical, and acoustical systems. The systems respond to an external forcing by developing a restoring force that re-establishes equilibrium in the system. A pendulum is a typical example of such a system. Free oscillations occur at the natural frequency of the system if the system disturbed beyond its equilibrium. Without additional forcing, these free oscillations retain the same frequencies but their amplitudes decay exponentially due to friction, until the system eventually comes to rest. In the case of a periodic continuous forcing, *forced* oscillations are produced with amplitudes depending on friction and the proximity of the forcing frequency to the natural frequency of the system.<sup>84</sup>

**9.2.1. Long and narrow channel**

Standing wave heights in a closed, long and narrow nonrotating rectangular basin of length,  $L$ , and uniform depth,  $H$ , have a simple trigonometric form<sup>35,95</sup>:

$$\zeta(x; t) = A \cos kx \cos \omega t, \tag{9.1}$$

where  $\zeta$  is the sea level elevation,  $A$  is the wave amplitude,  $x$  is the along-basin coordinate,  $t$  is time,  $k = 2\pi/\lambda$  is the wave number,  $\lambda$  is the wavelength,  $\omega = 2\pi/T$  is the angular wave frequency, and  $T$  is the wave period. The angular frequency and wave number (or the period and wavelength) are linked through the following well-known relationships:

$$\omega = kc, \tag{9.2a}$$

$$T = \frac{\lambda}{c}, \tag{9.2b}$$

where  $c = \sqrt{gH}$  is the long-wave phase speed and  $g$  is the gravitational acceleration.

The condition of no-flow through the basin boundaries ( $x = 0$ ;  $x = L$ ) yields the wave numbers:

$$k = \frac{\pi}{L}, \frac{2\pi}{L}, \frac{3\pi}{L}, \dots, \frac{n\pi}{L}, \tag{9.3}$$

which are related to the specific oscillation modes [Fig. 9.1(a)], i.e., to the various eigen modes of the water basin. The fundamental ( $n = 1$ ) mode has a wavelength equal to twice the length of the basin; a basin oscillating in this manner is known as a *half-wave oscillator*.<sup>34</sup> Other modes (*overtones* of the main or fundamental

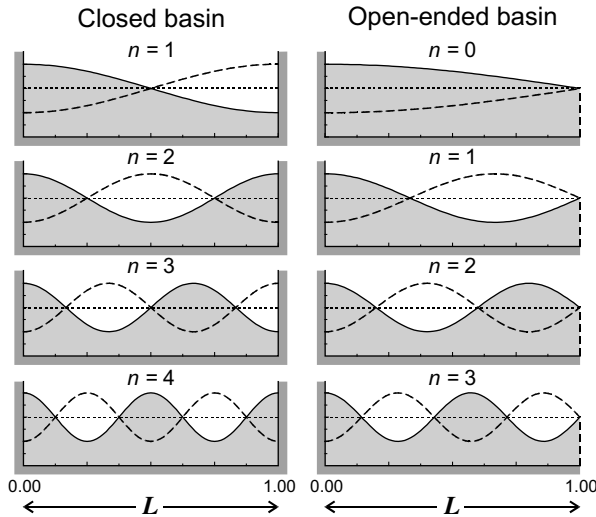


Fig. 9.1. Surface profiles for the first four seiche modes in closed and open-ended rectangular basins of uniform depth.

Table 9.1. Normalized periods,  $T_n^* = T_n \sqrt{gH}/(2L)$ , for a closed and open-mouth rectangular basin of uniform depth.

Basin	Mode				
	$n = 0$	$n = 1$	$n = 2$	$n = 3$	$n = 4$
Closed	—	1	1/2	1/3	1/4
Open-mouthed	2	2/3	2/5	2/7	2/9

“tone”) have wavelengths equal to one-half, one-third, one-fourth, and so on, of the wavelength of the fundamental mode (Fig. 9.1(a), Table 9.1).

The fundamental mode is antisymmetric: when one side of the water surface is going up, the opposite side is going down. Maximum sea level oscillations are observed near the basin borders ( $x = 0$ ;  $x = L$ ), while maximum currents occur at the *nodal lines*, i.e., the lines where  $\zeta = 0$  for all time. Positions of the nodal lines are determined by

$$x_n^m = \frac{(2m-1)L}{2n}, \quad m, n = 1, 2, \dots; \quad m \leq n. \quad (9.4)$$

Thus, for  $n = 1$ , there is one nodal line:  $x_1^1 = L/2$  located in the middle of the basin; for  $n = 2$ , there are two lines:  $x_2^1 = L/4$  and  $x_2^2 = 3L/4$ ; for  $n = 3$ :  $x_3^1 = L/6$ ,  $x_3^2 = 3L/6 = L/2$  and  $x_3^3 = 5L/6$  and so on. The number of nodal lines equals the mode number  $n$  [Fig. 9.1(a)], which is why the first mode is called the *uninodal* mode, the second mode is called *binodal* mode, the third mode the *trinodal* mode, etc.<sup>31,95</sup> The *antinodal* positions are those for which  $\zeta$  attains maximum values, and are specified as

$$x_n^j = \frac{jL}{n}, \quad j = 0, 1, 2, \dots, n. \quad (9.5)$$

For example, for  $n = 2$  there are three antinodal lines:  $x_2^0 = 0$ ,  $x_2^1 = L/2$ , and  $x_2^2 = L$ . Maximum currents occur at the nodal lines, while minimum currents occur at the antinodes. Water motions at the seiche nodes are entirely *horizontal*, while at the antinodes they are entirely *vertical*.

The relationships (9.2) and (9.3) yield the well-known *Merian's formula* for the periods of (natural) in a rectangular basin of uniform depth<sup>68,78</sup>:

$$T_n = \frac{2L}{n\sqrt{gH}}, \quad (9.6)$$

where  $n = 1, 2, 3, \dots$ . Merian's formula (9.6) shows that the longer the basin length ( $L$ ) or the shallower the basin depth ( $H$ ), the longer the seiche period. The fundamental ( $n = 1$ ) mode has the maximum period; other modes — the *overtone*s of the main fundamental — “tone” — have periods equal to one-half, one-third, one-fourth, and so on, of the fundamental period (Fig. 9.1(a), Table 9.1). The fundamental mode and all other odd modes are antisymmetric, while even modes are symmetric; an antinode line is located in the middle of the basin.

The structures and parameters of open-mouth basins are quite different from those of closed basins. Standing oscillations in a rectangular bay (harbor) with uniform depth and open entrance also have the form (9.1) but with a nodal line located near the entrance (bay mouth). In general, the approximate positions of nodal lines are determined by the following expressions (Fig. 9.1(b), Table 9.1):

$$x_n^m = \frac{(2m+1)L}{2n+1}, \quad m, n = 0, 1, 2, \dots; \quad m \leq n, \quad (9.7)$$

while antinodes are located at

$$x_n^j = \frac{2jL}{2n+1}, \quad j, n = 0, 1, 2, \dots; \quad j \leq n. \quad (9.8)$$

In particular, for  $n = 1$  there are two nodal lines:  $x_1^0 = L/3$  and  $x_1^1 = L$  and two antinodal lines:  $x_1^0 = 0$  and  $x_1^1 = 2L/3$ ; for  $n = 2$  there are three nodal lines:  $x_2^0 = L/5$ ,  $x_2^1 = 3L/5$  and  $x_2^2 = L$ , and three antinodal:  $x_2^0 = 0$ ,  $x_2^1 = 2L/5$ , and  $x_2^2 = 4L/5$ .

The most interesting and important mode is the lowest mode, for which  $n = 0$ . This mode, known as the *Helmholtz mode*, has a single nodal line at the mouth of the bay ( $x = L$ ) and a single antinode on the opposite shore ( $x = 0$ ). The wavelength of this mode is equal to four times the length of the bay; a basin oscillating in this manner is known as a *quarter-wave oscillator*.<sup>34</sup> The Helmholtz mode, which is also called the *zeroth mode*,<sup>a</sup> the *gravest mode* and the *pumping mode* (because it is related to periodic mass transport — pumping — through the open mouth,<sup>36,41</sup> is of particular importance for any given harbor. For narrow-mouthed bays and harbors, as well as for narrow elongated inlets and fjords, this mode normally dominates.

The periods of the Helmholtz and other harbor modes can be approximately estimated as<sup>84,95</sup>

$$T_n = \frac{4L}{(2n+1)\sqrt{gH}}, \quad \text{for mode } n = 0, 1, 2, 3, \dots \quad (9.9)$$

Using (9.9) and (9.6), the fundamental (Helmholtz) mode in a rectangular open-mouth basin of uniform depth  $H$  is found to have a period,  $T_0 = 4L/\sqrt{gH}$ , which is double the period of the gravest mode in a similar but closed basin,  $T_1 = 2L/\sqrt{gH}$ . Normalized periods of various modes (for  $n \leq 4$ ) are shown in Table 9.1.

Expressions (9.4)–(9.9), Table 9.1, and Fig. 9.1 are all related to the idealized case of a simple rectangular basin of uniform depth. This model is useful for some preliminary estimates of seiche parameters in closed and semi-closed natural and artificial basins. Analytical solutions can be found for several other basins of simple geometric form and nonuniform depth. Wilson<sup>95</sup> summarizes results that involve common basin shapes (Tables 9.2 and 9.3), which in many cases are quite

<sup>a</sup>In many papers and text books,<sup>8,94,95</sup> this mode is considered the “first mode”. However, it is more common to count nodal lines only inside the basin (not at the entrance) and to consider the fundamental harbor mode as the “zeroth mode”.<sup>41,68,78,80,84</sup> This approach is physically more sound because this mode is quite specific and markedly different from the first mode in a closed basin.

good approximations to rather irregular shapes of natural lakes, bays, inlets, and harbors.

The main concern for port operations and ships and boats in harbors is not from the sea level seiche variations but from the strong currents associated with the seiche. As noted above, maximum horizontal current velocities occur at the nodal lines. Therefore, its locations in the vicinity of the nodes that are potentially most risky and unsafe. Maximum velocities,  $V_{\max}$ , can be roughly estimated as<sup>84</sup>:

$$V_{\max} = A_n \sqrt{\frac{g}{H}}, \quad (9.10)$$

where  $A_n$  is the amplitude of the sea level oscillation for the mode. For example, if  $A_n = 0.5$  m and  $H = 6$  m,  $V_{\max} \approx 0.64$  m/s.

### 9.2.2. Rectangular and circular basins

If a basin is not long and narrow, the 1D approach used above is not appropriate. For such basins, 2D effects may begin to play an important role, producing compound or coupled seiches.<sup>95</sup> Two elementary examples, which can be used to illustrate the 2D structure of seiche motions, are provided by rectangular and circular basins of uniform depth ( $H$ ). Consider a rectangular basin with length  $L$  ( $x = 0, L$ ) and width  $l$  ( $y = 0, l$ ). Standing oscillations in the basin have the form<sup>35,41</sup>

$$\zeta(x, y; t) = A_{mn} \cos \frac{m\pi x}{L} \cos \frac{n\pi y}{l} \cos \omega t, \quad (9.11)$$

where  $m, n = 0, 1, 2, 3, \dots$ . The eigen wave numbers ( $k_{mn}$ ) are

$$k_{mn} = \left[ \left( \frac{m\pi}{L} \right)^2 + \left( \frac{n\pi}{l} \right)^2 \right]^{1/2}, \quad (9.12)$$

and the corresponding eigen periods are<sup>78</sup>

$$T_{mn} = \frac{2}{\sqrt{gh}} \left[ \left( \frac{m}{L} \right)^2 + \left( \frac{n}{l} \right)^2 \right]^{-1/2}. \quad (9.13)$$

For  $n = 0$  expression (9.13) becomes equivalent to the *Merian's formula* (9.6); the longest period corresponds to the *fundamental mode* ( $m = 1, n = 0$ ) which has one nodal line in the middle of the basin. In general, the numbers  $m$  and  $n$  denote the number of nodal lines across and along the basin, respectively. The normalized eigen periods  $T_{mn}^* = T_{mn}/T_{10}$  and spatial structure for the different modes are shown in Table 9.4.

For oscillations in a circular basin of radius  $r = a$ , it is convenient to use a polar coordinate system ( $r, \theta$ ) with the origin in the center:

$$x = r \cos \theta, \quad y = r \sin \theta,$$

where  $\theta$  is the polar angle. Standing oscillations in such basins have the form

$$\zeta(x, y; t) = J_s(kr)(A_s \cos s\theta + B_s \sin s\theta) \cos \omega t, \quad (9.14)$$

Table 9.2. Modes of free oscillations in closed basins of simple geometric shape and constant width (after Ref. 95).

Basin type		Profile equation	Periods of free oscillation				
Description	Dimensions		Fundamental $T_1$	Mode ratios $T_n/T_1$ values for $n$			
				1	2	3	4
Rectangular		$h(x) = h_0$	$2L/(gh_0)^{1/2}$	1.000	0.500	0.333	0.250
Triangular (isosceles)		$h(x) = h_0(1 - 2x/L)$	$1.305[2L/(gh_0)^{1/2}]$	1.000	0.628	0.436	0.343
Parabolic		$h(x) = h_0(1 - 4x^2/L^2)$	$1.110[2L/(gh_0)^{1/2}]$	1.000	0.577	0.408	0.316
Quartic		$h(x) = h_0(1 - 4x^2/L^2)^2$	$1.242[2L/(gh_0)^{1/2}]$	1.000	0.686	0.500	0.388

*(Continued)*



Table 9.2. (Continued)

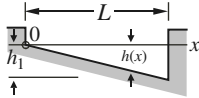
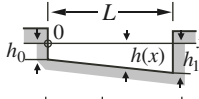
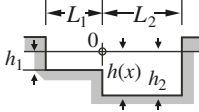
Basin type		Periods of free oscillation					
Description	Dimensions	Profile equation	Fundamental $T_1$	Mode ratios $T_n/T_1$ values for $n$			
				1	2	3	4
Triangular (right-angled)		$h(x) = h_1 x/L$	$1.640[2L/(gh_1)^{1/2}]$	1.000	0.546	0.377	0.288
Trapezoidal		$h(x) = h_0 + mx$ $m = (h_1 - h_0)/L$		1.000	0.546	0.377	0.288
Coupled, rectangular		$h(x) = h_1(x < 0)$ $h(x) = h_2(x > 0)$	$L_1/L_2 = 1/2 \quad 4L_2/(gh_2)^{1/2}$	1.000	0.500	0.250	0.125
		$h_1/h_2 = 1/4$	$L_1/L_2 = 1/3 \quad 3.13L_2/(gh_2)^{1/2}$	1.000	0.559	0.344	0.217
			$L_1/L_2 = 1/4 \quad 2.73L_2/(gh_2)^{1/2}$	1.000	0.579	0.367	0.252
		$L_1/L_2 = 1/8 \quad 2.31L_2/(gh_2)^{1/2}$	1.000	0.525	0.371	0.279	

Table 9.3. Modes of free oscillations in semi-closed basins of simple geometric shape (modified after Ref. 95).

Basin type		Periods of free oscillation					
Description	Dimensions	Profile equation	Fundamental $T_0$	Mode ratios $T_s/T_1$ [ $n = (s + 1)/2$ ]			
				$n = 0$	1	2	3
<p>Rectangular</p>	<p>Rectangular</p>	$h(x) = h_1$	$2.000[2L/(gh_1)^{1/2}]$	1.000	0.333	0.200	0.143
<p>Rectangular</p>	<p>Triangular</p>	$h(x) = h_1 x/L$	$2.618[2L/(gh_1)^{1/2}]$	1.000	0.435	0.278	0.203
<p>Rectangular</p>	<p>Semi-parabolic</p>	$h(x) = h_1(1 - x^2/L^2)$	$2.220[2L/(gh_1)^{1/2}]$	1.000	0.409	0.259	0.189
<p>Triangular</p>	<p>Rectangular</p>	$b(x) = b_1 x/L$ $h(x) = h_1$	$1.308[2L/(gh_1)^{1/2}]$	1.000	0.435	0.278	0.230

(Continued)

Table 9.3. (Continued)

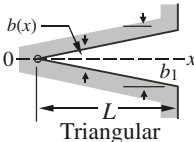
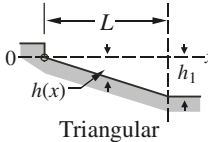
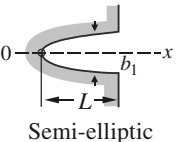
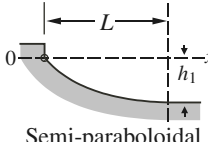
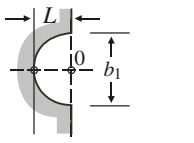
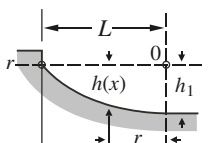

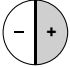

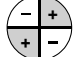
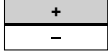
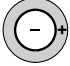

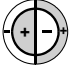




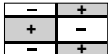

Basin type		Periods of free oscillation					
Description	Dimensions	Profile equation	Fundamental $T_0$	Mode ratios $T_s/T_1$ [ $n = (s + 1)/2$ ]			
				$n = 0$	1	2	3
 <p>Triangular</p>	 <p>Triangular</p>	$b(x) = b_1 x/L$ $h(x) = h_1 x/L$	$1.653[2L/(gh_1)^{1/2}]$	1.000	0.541	0.374	0.283
 <p>Semi-elliptical</p>	 <p>Semi-paraboloidal</p>	$b_1/L = 2$ $= 4/3$ $= 1$ $= 2/3$	$2.220[2L/(gh_1)^{1/2}]$	1.000	0.707 0.554 0.447 0.317	0.578 0.493 0.468 0.455	0.378 0.323 0.264 0.185
 <p>Semi-circular</p>	 <p>Semi-paraboloidal</p>	$h(x) = h_1(1 - r^2/L^2)$	$2.220[2L/(gh_1)^{1/2}]$	1.000	0.707	0.578	0.500

Table 9.4. Mode parameters for free oscillations in uniform depth basins of rectangular and circular geometric shape.

Rectangular basin ( $l = 0.5L$ )				Circular basin						
Mode numbers		Mode forms	Relative period	Mode numbers		Mode forms	Circular nodal lines		Normalized frequency	Relative period
$m$	$n$	$L$	$T_{mn}/T_{10}$	$s$	$m$	$2a$	$r_1$	$r_2$	$\omega a/c$	$T_{sm}/T_{10}$
1	0		1.000	1	0		—	—	1.841	1.000
2	0		0.500	2	0		—	—	3.054	0.603
0	1		0.500	0	1		0.628	—	3.832	0.480
1	1		0.447	1	1		0.719	—	5.331	0.345
2	1		0.354	2	1		0.766	—	6.706	0.275
0	2		0.250	0	2		0.343	0.787	7.016	0.262
1	2		0.243	1	2		0.449	0.820	8.536	0.216

where  $J_s$  is the Bessel function of an order  $s$ ,  $A_s$  and  $B_s$  are arbitrary constants, and  $s = 0, 1, 2, 3, \dots$ .<sup>35,41</sup> These oscillations satisfy the boundary condition:

$$J'_s(kr)|_{r=a} = J'_s(ka) = 0. \quad (9.15)$$

The roots of this equation determine the eigen values  $k_{sm}$  ( $m, s = 0, 1, 2, 3, \dots$ ), with corresponding eigen modes described by Eq. (9.14) for various  $k = k_{sm}$ . Table 9.4 presents the modal parameters and the free surface displacements of particular modes.

As illustrated by Table 9.4, there are two classes of nodal lines, “rings” and “spokes” (diameters). The corresponding mode numbers  $m$  and  $s$  give the respective exact number of these lines. Due to mass conservation, the mode  $(0, 0)$  does not exist in a completely closed basin.<sup>41</sup> For the case  $s = 0$ , the modes are symmetrical with respect to the origin and have annular crest and troughs.<sup>35</sup> In particular, the first symmetrical mode ( $s = 0, m = 1$ ) has one nodal ring  $r = 0.628a$  (Table 9.4). When the central part of the circular basin (located inside of this ring) is going up, the marginal part (located between this ring and the basin border) is going down, and *vice versa*. The second symmetrical mode ( $s = 0, m = 2$ ) has two nodal rings:  $r = 0.343a$  and  $r = 0.787a$ .

For  $s > 0$ , there are  $s$  equidistant nodal diameters located at an angle  $\Delta\theta = \pi/s$  from each other; i.e.,  $180^\circ$  for  $s = 1$ ,  $90^\circ$  for  $s = 2$ ,  $60^\circ$  for  $s = 3$ , etc. Positions of these diameters are indeterminate, since the origin of  $\theta$  is arbitrary. The indeterminability disappears if the boundary deviates even slightly from a circle. Specifically, the first nonsymmetrical mode ( $s = 1, m = 0$ ) has one nodal diameter ( $\theta = \pi/2$ ), whose position is undefined; but if the basin is not circular but elliptical, the nodal line would coincide with either the major or minor axis, and the corresponding eigen periods would be unequal.<sup>35</sup> The first unsymmetrical mode has the lowest frequency and the largest eigen period (Table 9.4); in this case, the water sways from one side to another relative to the nodal diameter. This mode is often referred to as the “sloshing” mode.<sup>78</sup>

Most natural lakes or water reservoirs can support rather complex 2D seiches. However, the two elementary examples of rectangular and circular basins help to understand some general properties of the corresponding standing oscillations and to provide rough estimates of the fundamental periods of the basins.

### 9.2.3. Harbor resonance

Let us return to harbor oscillations and consider some important resonant properties of semi-closed basins. First, it is worthy to note that expressions (9.7)–(9.9) and Table 9.3 for open-mouth basins give only approximate values of the eigen periods and other parameters of harbor modes. Solutions of the wave equation for basins of simple geometric forms are based on the boundary condition that a nodal line (zero sea level) is always *exactly at the entrance* of a semi-closed basin that opens onto a much larger water body. In this case, the free harbor modes are equivalent to odd (antisymmetric) modes in a closed basin, formed by the open-mouth basin and its

mirror image relative to the mouth.<sup>b</sup> However, this condition is not strictly correct because it does not take into account wave energy radiation through the mouth into the open sea. The exact solutions may be obtained based on the *Sommerfeld radiation condition* of free wave radiation through the open boundary.<sup>35,41</sup> Following application of the appropriate *mouth correction* ( $\alpha$ ), the nodal line is located close to but *outside the entrance*. In other words, the effect of this correction is to increase the effective length of the basin.<sup>95</sup> The mouth correction depends on two parameters: the basin aspect ratio  $q = l/L$ , which relates the width of the basin ( $l$ ) to its length ( $L$ ); and the aperture ratio  $\vartheta = b/l$ , in which  $b$  is the actual width of the mouth.

Mathematical determination of  $\alpha$  is rather complicated but, as a rule, it increases with increases of  $q$  and  $\vartheta$ . For example, the fractional correction to Eq. (9.9) for the fundamental mode in a rectangular basin of uniform depth and open mouth ( $\vartheta = 1.0$ ) is determined as<sup>30,95</sup>

$$\alpha = \left(\frac{q}{\pi}\right) \left[\frac{3}{2} - \gamma - \ln\left(\frac{\pi q}{4}\right)\right], \quad (9.16)$$

where  $\gamma = 0.5772$  is Euler's constant. Roughly speaking, radiation into the external basin and the mouth correction are important when the semi-closed basin is broad and has a large open entrance, and negligible when the basin is long and narrow (i.e., when  $q$  is small); in the latter case, expressions (9.7)–(9.9), as well as those presented in Table 9.3, are quite accurate.

The character of natural oscillations in a bay or harbor is strongly controlled by the aperture ratio  $\vartheta = b/l$ , which can vary from  $\vartheta = 1.0$  to  $\vartheta = 0.0$ . These two asymptotic cases represent a fully open harbor and a closed basin, respectively. It is evident that the smaller is  $\vartheta$  (i.e., the smaller the width of the entrance), the slower water from the external basin (open sea) penetrates into the harbor. Thus, as  $\vartheta$  decreases, the periods of all harbor modes for  $n \geq 1$  in Table 9.1 increase, tending to the periods of the corresponding eigen modes for a closed basin, while the period of the fundamental (Helmholtz) harbor mode tends to infinity.<sup>c</sup> This is one of the important properties of harbor oscillations.

Another important property is harbor resonance. The amplification factor for long waves impinging on a harbor from the open sea is

$$H^2(f) = \frac{1}{(1 - f/f_0)^2 + Q^{-2}(f/f_0)^2}, \quad (9.17)$$

where  $f$  is the frequency of the long incoming waves,  $f_0$  is the resonant frequency of the harbor, and  $Q$  is the quality factor (“ $Q$ -factor”), which is a measure of energy damping in the system.<sup>47,95</sup> Specifically,

$$Q^{-1} = \frac{dE/dt}{\omega E} = 2\beta, \quad (9.18)$$

<sup>b</sup>This approach is used for numerical computation of eigen modes in natural 2D basins.<sup>70</sup>

<sup>c</sup>This is the reason for calling this the “zeroth mode.”

where  $E = E_0 e^{-2\beta\omega t}$  is the energy of the system as it decays from an initial value  $E_0$ ,  $\beta$  is a dimensionless damping coefficient, and  $\omega = 2\pi f$  is the angular frequency. The power amplification factor attains the value  $Q^2$  at resonance ( $f = f_0$ ), decreases to unity at  $f = 0$  and goes to zero as  $f$  goes to infinity. Therefore,  $Q$  for harbor oscillations plays a double role: as a measure of the resonant increase of wave heights for waves arriving from the open ocean and as an index of the time decay rate of wave heights inside the harbor. The higher the  $Q$ , the stronger will be the amplification of the incoming waves and the slower the energy decay, i.e., the longer the “ringing” of seiche oscillations inside the harbor.

In closed basins, like lakes, bottom friction is the main factor controlling energy decay. Normally, it is quite small, so in lakes with fairly regular topographic features (low damping), a high  $Q$ -factor may be expected. Consequently, even a small amount of forcing energy at the resonant frequency can produce significant seiche oscillations that persist for several days.<sup>31,95</sup> In contrast, the main factor of energy decay in semi-closed water basins, such as gulfs, bays, fjords, inlets and harbors, is wave radiation through the entrance. In their pioneering work, Miles and Munk<sup>47</sup> concluded that narrowing the harbor entrance would increase the quality factor  $Q$  and, consequently, the amplification of the arriving wave. This means that the construction of dams, dikes, and walls to protect the harbor from wind waves and swell could so constrict the entrance width that it leads to strong amplification of the resonant seiche oscillations inside the harbor. Miles and Munk<sup>47</sup> named this *harbor paradox*.

As pointed out by Miles and Munk,<sup>47</sup> there are two limitations to the previous conclusions:

(1) A time of order  $Q/\pi$  cycles is necessary for the harbor oscillations to adjust to the external forcing. This means that harbors with high  $Q$  would not respond to a strong but short-lived incoming disturbance. In most cases, this limitation is not of major concern because atmospheric disturbances (the major source of open-sea long waves inducing harbor oscillations) are likely to last at least for several hours. Even tsunami waves from distant locations “ring” for many hours, resonantly “feeding” harbor seiches and producing maximum oscillations that have long (12–30 h) durations that persist well after the arrival of the first waves.<sup>74,75</sup> This contrasts with the case for near-field sites, where tsunamis normally arrive as short-duration impulsive waves. Such tsunamis are much more dangerous at open coastal regions than in bays or harbors, as was observed for the coast of Thailand after the 2004 Sumatra tsunami.<sup>86</sup>

(2) As the harbor mouth becomes increasingly narrower, the internal harbor dissipation eventually exceeds energy radiation through the mouth. At this stage, further narrowing does not lead to a further increase in the  $Q$ -factor. However, normally internal dissipation is small compared to the typical radiative energy losses through the entrance.

Originally, Miles and Munk<sup>47</sup> believed that their “harbor paradox” concept was valid for every harbor mode provided the corresponding spectral peak was sharp and well defined. Further thorough examination of this effect<sup>37,46,78</sup> indicated that the harbor paradox is only of major importance for the Helmholtz mode, while for higher modes frictional and nonlinear factors, not accounted for in the theory,

dampen this effect.<sup>95</sup> However, the Helmholtz mode is the most important mode in natural basins and is normally observed in bays, inlets, and harbors with narrow entrance, i.e., in semi-closed basins with high  $Q$ -factor. Significant problems with the mooring and docking of ships (and the loading and unloading of their cargo) in ports and harbors are often associated with this fundamental mode and most typically occur in ports with high  $Q$ .<sup>4,6,41,62,66–68,78–80</sup>

Rabinovich<sup>67</sup> suggested reducing these negative effects in ports by artificially increasing the internal dissipation. The idea is the same as that widely used in rocket technology to damp eigen oscillations in fuel tanks.<sup>44,45</sup> Radial piers in ports and harbors play the same role as internal rings and ribs in rocket tanks, efficiently transforming wave energy into vortical motions which reduce the wave energy and therefore the intensity of the seiches and their associated horizontal currents. As shown by Rabinovich,<sup>67</sup> the logarithmic attenuation factor,  $\delta_0 = \pi/Q$ , for the Helmholtz mode associated with the  $j$ th pier, is given by

$$\delta_0^j = \frac{\Delta E_0^j}{2E_0} = \frac{1}{6} C_x^j \left( \frac{b_j}{r_0} \right) \left( \frac{\hat{\xi}_0}{h_0} \right) \left( \frac{\omega_0}{\sigma_0} \right), \quad (9.19)$$

where  $E_0$  is the energy of the mode inside the harbor,  $\Delta E_0^j$  is the energy dissipated at the pier over the mode period ( $T_0 = 2\pi/\omega_0$ ),  $b_j$  is the length of the pier,  $r_0$  and  $h_0$  are the mean radius and depth of the harbor,  $\hat{\xi}_0$  is the mean amplitude of the Helmholtz mode in the harbor,  $C_x^j$  is a dimensionless resistance coefficient, and  $\sigma_0 = (gh_0)^{1/2}/(\pi r_0)$ . Thus, the rate of damping of oscillations in a harbor depends on the number of piers ( $N$ ) and a number of dimensionless parameters: specifically, the relative amplitudes of the oscillations,  $\xi_0 = \hat{\xi}_0/h_0$ ; the normalized harbor frequency,  $\Omega_0 = \omega_0/\sigma_0$ ; the relative lengths of the piers,  $B_j = b_j/r_0$ ; and the coefficient  $C_x^j$ . The parameter  $\xi_0$  depends on the intensity of the external forcing while the two other parameters  $\Omega_0$  and  $B_j$  do not depend on forcing but only on the characteristics of the harbor. The coefficient  $C_x^j$  strongly depends on the Keulegan–Carpenter (KC) number which relates hydraulic resistance in oscillating flows to those for stationary currents.<sup>32</sup> For typical values  $B_j = 0.3$ ,  $\xi_0 = 0.1$ ,  $\Omega_0 = 1.0$ ,  $N = 8$ , and  $C_x^j = 10$ , we find  $\delta_0 \approx 0.4$  and  $Q \approx 8$ .

Another important aspect of the harbor oscillation problem is that changes in port geometry, and the construction of additional piers and dams can significantly change the natural (eigen) periods of the port, thereby modifying considerably the resonant characteristics of the basin.<sup>6</sup> Helmholtz resonators in acoustics are used to attenuate sound disturbances of long wavelengths, which are difficult to reduce using ordinary methods of acoustical energy dissipation. Similarly, side channel resonators are suggested as a method for attenuating incident wave energy in harbors.<sup>6,66,78</sup>

In general, estimation of the  $Q$ -factor is a crucial consideration for ports, harbors, bay, and inlets. For a rectangular basin of uniform depth and entirely open mouth ( $\vartheta = b/l = 1.0$ ), this factor is easily estimated as:

$$Q = \frac{L}{l}, \quad (9.20)$$

which is inversely proportional to the aspect ratio  $q = l/L$ . This means that high  $Q$ -factors can be expected for long and narrow inlets, fjords, and waterways.



Honda *et al.*<sup>30</sup> and Nakano and Unoki<sup>59</sup> examined coastal seiches at more than 110 sites on the coast of Japan and found that strong and highly regular seiche oscillations are most often observed in such elongated basins and that the periods of these oscillations are in good agreement with the approximate period (9.9) for the Helmholtz mode ( $n = 0$ ):

$$T_0 = \frac{4L}{\sqrt{gH}} . \quad (9.21)$$

If the aperture ratio  $\vartheta < 1.0$ , corresponding to a partly closed entrance, it is more difficult to estimate the  $Q$  value and the resonant mode periods analytically. In practice, special diagrams for a rectangular basin with various  $q$  and  $\vartheta$  are used for these purposes.<sup>80,84</sup> For natural basins, these parameters can be estimated numerically or from direct observations. If the respective spectral peak in observational data is isolated, sharp and pronounced enough, then we can assume that  $Q \gg 1$ . In this case, it follows from (9.17) that the half-power frequency points ( $f_{1/2}$ ) are given by the following expression<sup>47</sup>:

$$f_{1/2}^{\pm} = f_0 \left( 1 \pm \frac{1}{2Q} \right) , \quad (9.22)$$

and the relative frequency bandwidth is simply

$$\frac{\Delta f}{f_0} = Q^{-1} , \quad (9.23)$$

where  $\Delta f = f_{1/2}^+ - f_{1/2}^-$  and  $f_0 = 1/T_0$  is the resonant frequency. This is a useful practical method for estimating the  $Q$ -factor and amplification for coastal basins based on results of spectral analysis of observational data. However, the spatial structure of different modes, the distribution of currents, and sea levels inside a natural basin, influence harbor reconstruction based on changes in these characteristics, and many other aspects of harbor hydrodynamics, are difficult to estimate without numerical computations. Numerical modeling has become a common approach that is now widely used to examine harbor oscillations.<sup>4,14,70,92</sup>

#### 9.2.4. Harbor oscillations in a natural basin

Some typical features of harbor oscillations are made more understandable using a concrete example. Figures 9.2 and 9.3 illustrate properties of typical harbor oscillations and results of their analysis and numerical modeling. Several temporary cable bottom pressure stations (BPS) were deployed in bays on the northern coast of Shikotan Island, Kuril Islands in 1986–1992.<sup>13,14,68,70</sup> All BPSs were digital instruments that recorded long waves with 1-min sampling. One of these stations (BPS-1) was situated at the entrance of False Bay, a small bay with a broad open mouth [Fig. 9.2(a)]. The oscillations recorded at this site were weak and irregular; the respective spectrum [Fig. 9.2(b)] was “smooth” and did not have any noticeable peaks, probably because of the closeness of the instrument position to the position of the entrance nodal line. Two more gauges (BPS-2 and BPS-3) were located inside Malokurilsk Bay, a “bottle-like” bay with a maximum width of about

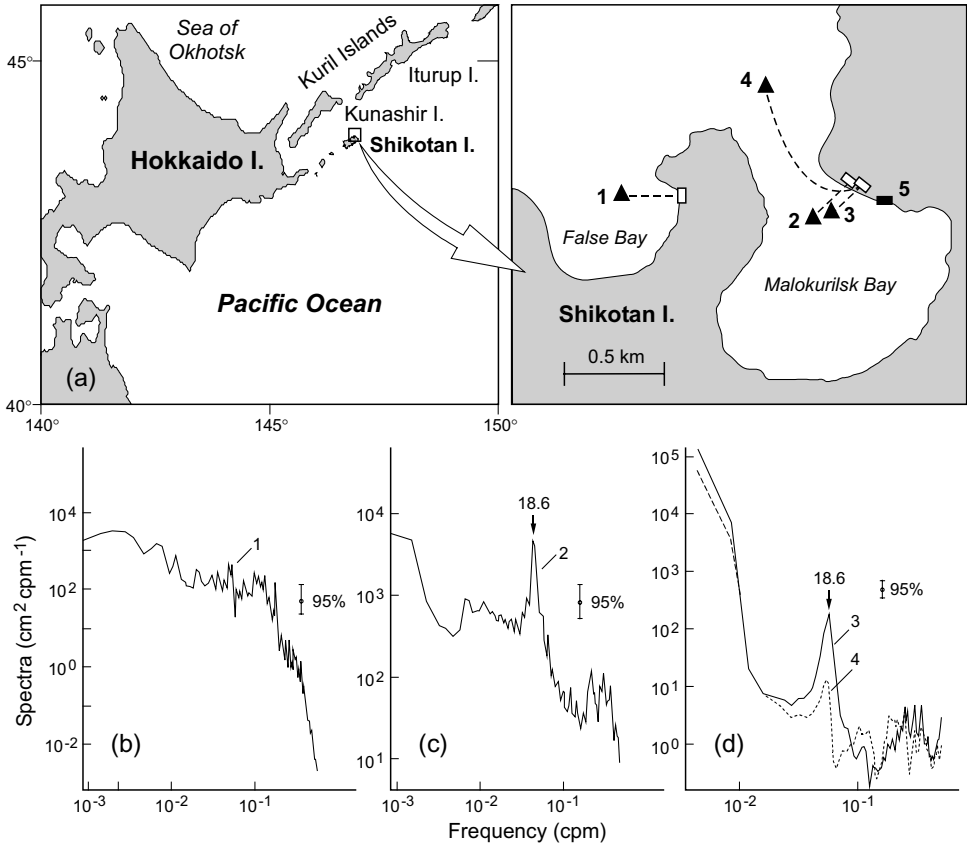


Fig. 9.2. (a) Location of cable bottom pressure stations near the northern coast of Shikotan Island (Kuril Islands) and sea level spectra at (b) BPS-1, (c) BPS-2 (both in autumn 1986) and (d) BPS-3 and BPS-4 (October–November 1990).

1300 m and a narrow neck of 350 m [Fig. 9.2(a)]. The oscillations recorded by these instruments were significant, highly regular and almost monochromatic; the corresponding spectra [Figs. 9.2(c) and 9.2(d)] have a prominent peak at a period of 18.6 min. An analogue tide gauge [#5 in Fig. 2(a)] situated on the coast of this bay permanently measure oscillations with exactly the same period.<sup>70</sup> It is clear that this period is related to the fundamental mode of the bay. The  $Q$ -factor of the bay, as estimated by expression (9.23) based on spectral analysis of the tide gauge data for sites BPS-2 and BPS-3, was 12–14 and 9–10, respectively. The high  $Q$ -factors are likely the main reason for the resonant amplification of tsunami waves that arrive from the open ocean. Such tsunami oscillations are regularly observed in this bay.<sup>13,69</sup> In particular, the two recent Kuril Islands tsunamis of 15 November 2006 and 13 January 2007 generated significant resonant oscillations in Malokurilsk Bay of 155 cm and 72 cm, respectively, at the same strongly dominant period of 18.6 min.<sup>76</sup>

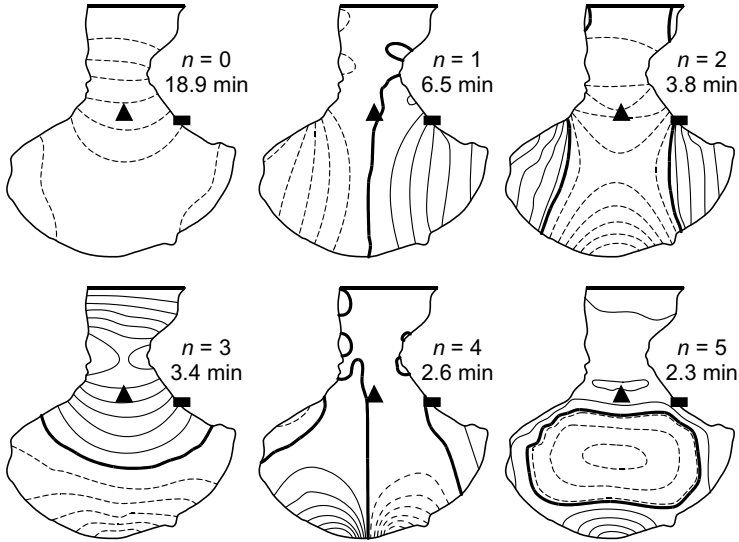


Fig. 9.3. Computed eigen modes and periods of the first six modes in Malokurilsk Bay (Shikotan Island). Black triangles indicate positions of the BPS-2 and BPS-3 gauges (from Ref. 70).

Figure 9.3 shows the first six eigen modes for Malokurilsk Bay.<sup>70</sup> The computations were based on numerical conformal mapping of the initial mirror reflected domain on a circular annulus (for details, see Ref. 77) and the following application of Ritz's variational method to solve the eigenvalue problem. The computed period of the fundamental (Helmholtz) mode (18.9 min) was close to the observed period of 18.6 min. The spectra at BPS-2 and BPS-2 indicate weak spectral peaks (three orders of magnitude less than the main peak) with periods 4.1, 3.3, and 2.9 min (the latter only at BPS-3), thought to be related to modes  $n = 2, 3$ , and 4. The first mode ( $n = 1$ ), with period of 6.5 min, was not observed at these sites apparently because the nodal line for this mode passes through the positions of BPS-2 and BPS-3.

Thus, the computed periods of the bay eigen modes are in good agreement with observation; plots in Fig. 9.3 give the spatial structure of the corresponding modes. However, this approach does not permit direct estimation of the bay response to the external forcing and the corresponding amplification of waves arriving from the open ocean. In actuality, the main purpose of the simultaneous deployments at sites BPS-3 and BPS-4 [Fig. 9.2(a)] in the fall of 1990 was to obtain observed response parameters that could be compared with numerically evaluated values.<sup>14</sup> The spectrum at BPS-4, the station located on the outer shelf of Shikotan Island near the entrance to Malokurilsk Bay [Fig. 9.2(d)], contains a noticeable peak with period of 18.6 min associated with energy radiation from the bay. This peak is about 1.5 orders of magnitude lower than a similar peak at BPS-3 inside the bay. The amplification factor for the 18.6 min period oscillation at BPS-4 relative to that at BPS-3 was found to be about 4.0. Numerical computations of the response characteristics for Malokurilsk Bay using the HN-method<sup>14</sup> gave resonant periods which

were in close agreement with the empirical results of Rabinovich and Levyant<sup>70</sup> (indicated in Fig. 9.3). Resonant amplification of tsunami waves impinging on the bay was found to be 8–10.

### 9.2.5. *Seiches in coupled bays*

A well-known physical phenomenon are the oscillations of two simple coupled pendulums connected by a spring with a small spring constant (weak coupling). For such systems, the oscillation energy of the combined system systematically moves from one part of the system to the other. Every time the first pendulum swings, it pulls on the connecting string and gives the second pendulum a small tug, so the second pendulum begins to swing. As soon as the second pendulum starts to swing, it begins pulling back on the first pendulum. Eventually, the first pendulum is brought to rest after it has transferred all of its energy to the second pendulum. But now the original situation is exactly reversed, and the first pendulum is in a position to begin “stealing” energy back from the second. Over time, the energy repeatedly switches back and forth until friction and air resistance eventually remove all of the energy out of the pendulum system.

A similar effect is observed in two adjacent bays that constitute a coupled system. Nakano<sup>56</sup> was probably the first to investigate this phenomenon based on observations for Koaziro and Moroiso bays located in the Miura Peninsula in the vicinity of Tokyo. The two bays have similar shapes and nearly equal eigen periods. As was pointed out by Nakano, seiches in both bays are very regular, but the variations of their amplitudes are such that, while the oscillations in one bay become high, the oscillations in the other become low, and *vice versa*. Nakano<sup>56</sup> explained the effect theoretically as a coupling between the two bays through water flowing across the mouths of each bay. More than half a century later Nakano returned to this problem<sup>60</sup> and, based on additional theoretical studies and hydraulic model experiments, demonstrated that two possible regimes can exist in the bays: (1) *co-phase* oscillations when seiches in the two bays have the same initial phase; and (2) *contra-phase* when they have the opposite phase. The superposition of these two types of oscillations create *beat* phenomenon of time-modulated seiches, with the opposite phase modulation, such that “while one bay oscillates vigorously, the other rests”. Nakano and Fujimoto suggested the term “*liquid pendulums*” for the coupled interaction of two adjacent bays.

A more complicated situation occurs when the two adjacent bays have significantly different eigen periods. For example, Ciutadella and Platja Gran are two elongated inlets located on the west coast of Menorca Island, one of the Balearic Islands in the Western Mediterranean [the inlets are shown in the inset of Fig. 9.5(a)]. Their fundamental periods ( $n = 0$ ) are 10.5 min and 5.5 min, respectively.<sup>50,71,73</sup> As a result of the interaction between these two inlets, their spectra and admittance functions have, in addition to their “own” strong resonant peaks, secondary “alien” peaks originating from the other inlet.<sup>38</sup> This means that the mode from Ciutadella “spills over” into Platja Gran and *vice versa*. The two inlets are regularly observed to experience destructive seiches, locally known as “*rissaga*”.<sup>18,22,49–51,85</sup> Specific aspects of rissaga waves will be discussed later (in

Sec. 9.4); however, it is worth noting here that the coupling between the two inlets can apparently amplify the destructive effects associated with each of the inlets individually.<sup>38</sup>

### 9.3. Generation

Because they are natural resonant oscillations, seiches are generated by a wide variety of mechanisms (Fig. 9.4), including tsunamis,<sup>14,28,54,69</sup> seismic ground waves,<sup>2,15,34,40</sup> internal ocean waves,<sup>8,19,21</sup> and jet-like currents.<sup>30,54,57</sup> However, the two most common factors initiating these oscillations in bays and harbors are atmospheric processes and nonlinear interaction of wind waves or swell (Fig. 9.4).<sup>62,68,95</sup> Seiches in lakes and other enclosed water bodies are normally generated by direct external forcing on the sea surface, primarily by atmospheric pressure variations and wind.<sup>31,95</sup> In contrast, the generation of harbor oscillations is a two-step process involving the generation of long waves in the open ocean followed by forcing of the

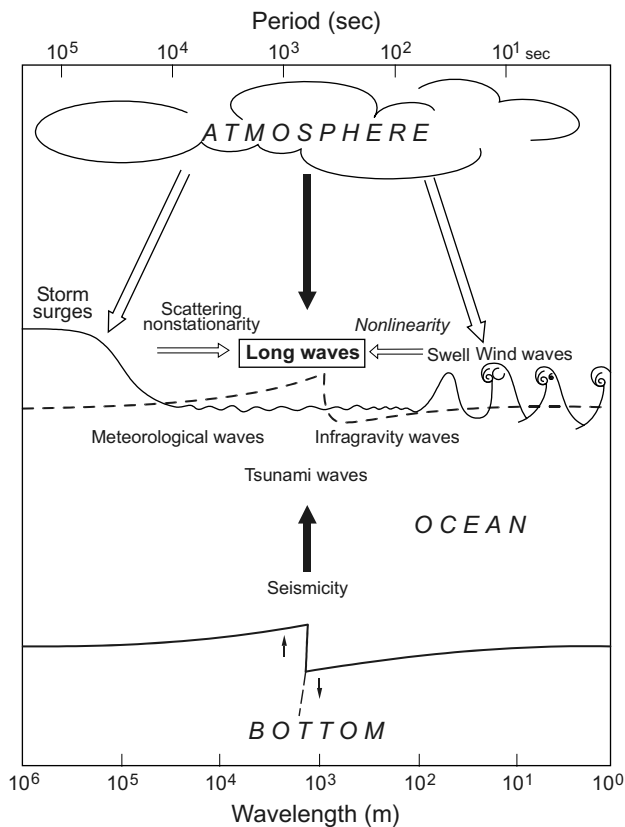


Fig. 9.4. Sketch of the main forcing mechanisms generating long ocean waves.

harbor oscillations as the long waves arrive at the harbor entrance where they lead to resonant amplification in the basin.

Seiche oscillations produced by external periodic forcing can be both free and forced. The free oscillations are true seiches (i.e., eigen oscillations of the corresponding basin). However, if the external frequency ( $\sigma$ ) differs from the eigen frequencies of the basin ( $\sigma \neq \omega$ ), the oscillations can be considered *forced seiches*.<sup>95</sup> Open-ocean waves arriving at the entrance of a specific open-mouth water body (such as a bay, gulf, inlet, fjord, or harbor) normally consist of a broad frequency spectrum that spans the response characteristics of the water body from resonantly generated eigenfree modes to nonresonantly forced oscillations at other frequencies. Following cessation of the external forcing, forced seiches normally decay rapidly, while free modes can persist for a considerable time.

Munk<sup>53</sup> jokingly remarked that “*the most conspicuous thing about long waves in the open ocean is their absence.*” This is partly true: the long-wave frequency band, which is situated between the highly energetic tidal frequencies and swell/wind wave frequencies, is relatively empty (Fig. 9.5). For both swell/wind waves and tides, the energy is of order  $10^4 \text{ cm}^2$ , while the energy contained throughout the entire intermediary range of frequencies is of order  $1\text{--}10 \text{ cm}^2$ . However, this particular frequency range is of primary scientific interest and applied importance (Walter Munk himself spent approximately 30 years of his life working on these “absent” waves!). Long waves are responsible for formation and modification of the coastal zone and shore morphology;<sup>5,68</sup> they also can strongly affect docking and loading/unloading of ships and construction in harbors, causing considerable damage.<sup>41,78,79,96</sup> Finally,

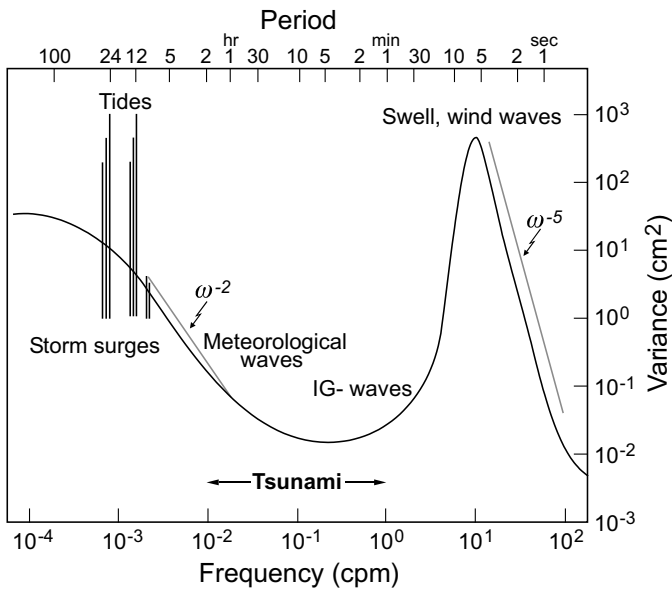


Fig. 9.5. Spectrum of surface gravity waves in the ocean (modified from Ref. 68). Periods (upper scale) are in hours (h), minutes (min), and seconds (s).

and probably the most important, are tsunamis and other marine hazardous long waves, which are related to this specific frequency band. The recent 2004 Sumatra tsunami in the Indian Ocean killed more than 226,000 people, triggering the largest international relief effort in history and inducing unprecedented scientific and public interest in this phenomenon and in long waves in general.<sup>86</sup>

Because of their resonant properties, significant harbor seiches can be produced by even relatively weak open ocean waves. In harbors and bays with high  $Q$ -factors, seiches are observed almost continuously. However, the most destructive events occur when the incoming waves have considerable energy at the resonant frequencies, especially at the frequency of the fundamental mode. Such a situation took place in Port Alberni located in the head of long Alberni Inlet on Vancouver Island (Canada) during the 1964 Alaska tsunami, when resonantly generated seiche oscillations in the inlet had trough-to-crest wave heights of up to 8 m, creating total economic losses of about \$10 million (1964 dollars).<sup>28,54</sup>

### 9.3.1. Meteorological waves

Long waves in the ocean are the primary factor determining the intensity of harbor oscillations. If we ignore tsunamis and internal waves, the main source of background long waves in the ocean are atmospheric processes (Fig. 9.4).<sup>10,53</sup> There are three major mechanisms to transfer the energy of atmospheric processes into long waves in the ocean<sup>68</sup>:

- (1) Direct generation of long waves by atmospheric forcing (pressure and wind) on the sea surface.
- (2) Generation of low-frequency motions (for example, storm surges) and subsequent transfer of energy into higher frequencies due to nonlinearity, topographic scattering and nonstationarity of the resulting motions.
- (3) Generation of high-frequency gravity waves (wind waves and swell) and subsequent transfer of energy into larger scale, lower frequency motions due to nonlinearity.

Long waves generated by the first two mechanisms are known as atmospherically induced or *meteorological waves*.<sup>d</sup> Typical periods of these waves are from a few minutes to several hours, typical scales are from one to a few hundreds of kilometers. The first mechanism is the most important because it is this mechanism that is responsible for the generation of destructive seiche oscillations (*meteorological tsunamis*) in particular bays and inlets of the World Ocean (Sec. 9.4). “Meteorological waves” can be produced by the passages of typhoons, hurricanes or strong cyclones. They also have been linked to frontal zones, atmospheric pressure jumps, squalls, gales, wind gusts and trains of atmospheric buoyancy waves.<sup>10,59,68,71,87,95</sup> The most frequent sources of seiches in lakes are barometric fluctuations. However they can also be produced by heavy rain, snow,

---

<sup>d</sup>The Russian name for these waves is “*anemobaric*”<sup>68</sup> because they are induced by atmospheric pressure (“*baric*”) and wind (“*anemos*”) stress forcing on the ocean surface.

or hail over a portion of the lake, or flood discharge from rivers at one end of the lake.<sup>27,31,95</sup>

### 9.3.2. *Infragravity waves*

Long waves generated through the nonlinear interaction of wind waves or swell are called *infragravity waves*.<sup>5,63</sup> These waves have typical periods of 30 s to 300–600 s and length scales from 100 m to 10 km. The occurrence of relatively high-frequency long waves, highly correlated with the modulation of groups of wind or swell waves, was originally reported by Munk<sup>52</sup> and Tucker.<sup>89</sup> Because the waves were observed as sea level changes in the nearshore surf zone, they became known as *surf beats*. Later, it was found that these waves occur anywhere there are strong nonlinear interacting wind waves. As a result, the more general term *infragravity waves* (proposed by Kinsman<sup>33</sup>) became accepted for these waves. Recent field measurements have established that infragravity waves (IG waves) dominate the velocity field close to the shore and consist of superposition of free *edge* waves propagating along the shore, free *leaky* waves propagating in the offshore direction, and forced *bound* waves locked to the groups of wind waves or swell propagating mainly onshore.<sup>3,5,68</sup> Bound IG waves form the set-down that accompanies groups of incident waves, having troughs that are beneath the high short waves of the group and crests in-between the wave groups.<sup>39</sup> They have the same periodicity and the same lengths as the wave groups and travel with the group velocity of wind waves, which is significantly smaller than the phase speed of free long waves with the same frequencies. Free edge IG waves arise from the trapping of swell/wind wave generated oscillations over sloping coastal topography, while free leaky waves are mainly caused by the reflection of bound waves into deeper water.<sup>5,63</sup> The general mechanisms of the formation of IG waves are shown in Fig. 9.6.<sup>e</sup>

IG waves are found to be responsible for many phenomena in the coastal zone, including formation of *rip currents*, *wave setup*, *crescentic bars*, *beach cusps* and other regular forms of coastal topographies, as well as transport of sediment materials. Being of high-frequency relative to meteorological waves, IG waves can induce seiches in comparatively small-scale semi-closed basins, such as ports and harbors, which have natural periods of a few minutes and which may pose a serious threat for large amplitude wave responses.

Certain harbors and ports are known to have frequent strong periodic horizontal water motions. These include Cape Town (South Africa), Los Angeles (USA), Dakar (Senegal), Toulon and Marseilles (France), Alger (Algeria), Tuapse and Sochi (Russia), Batumi (Georgia) and Esperance (Australia). Seiche motions in these basins create unacceptable vessel movement which can, in turn, lead to the breaking of mooring lines, fenders and piles, and to the onset of large amplitude ship oscillations and damage.<sup>62,67,68,82,94–96</sup> Known as *surging* or *range action*,<sup>78,79</sup> this phenomenon has well-established correlations with (a) harbor oscillations, (b) natural oscillations of the ship itself, and (c) intensive swell or wind waves outside the

<sup>e</sup>Figure 9.6 does not include all possible types of IG waves and mechanisms of their generation; a more detailed description is presented by Bowen and Huntley<sup>5</sup> and Battjes.<sup>3</sup>



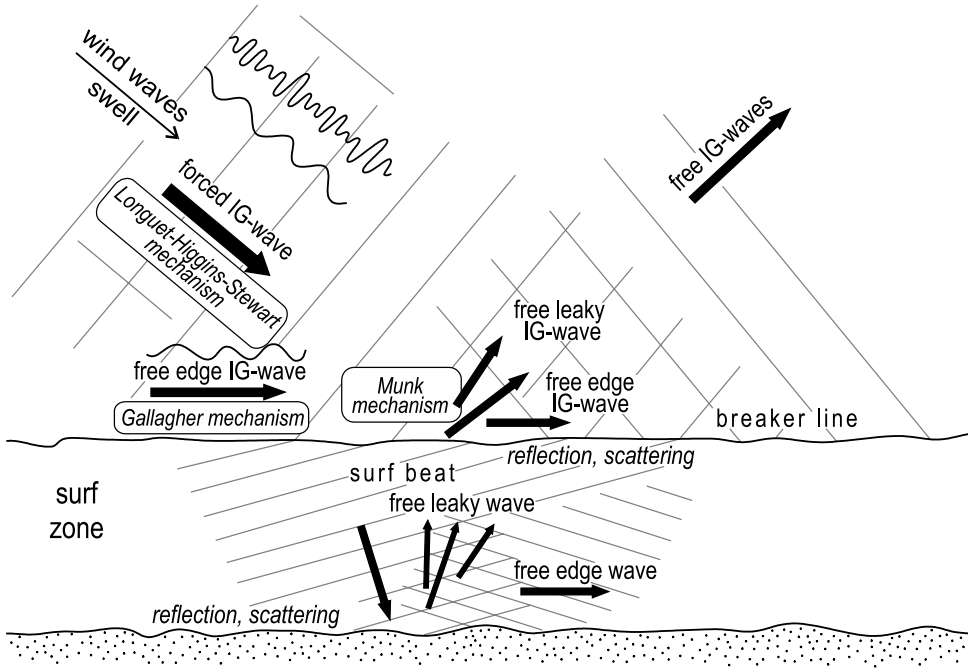


Fig. 9.6. Generation mechanisms for infragravity waves in the coastal zone.

harbor. Typical eigen periods of a harbor or a moored ship are the order of minutes. Therefore, they cannot be excited directly by wind waves or swell, having typical periods on the order of seconds.<sup>96</sup> However, these periods exactly coincide with the periods of wave groups and IG waves. So, it is conventional wisdom that surging in harbors is the result of a triple resonance of external oscillations outside the harbor, natural oscillations within the harbor, and natural oscillations of a ship. The probability of such triple resonance is not very high, thus surging occurs only in a limited number of ports. Ports and harbors having large dimensions and long eigen periods ( $>10$  min) are not affected by surging because these periods are much higher than the predominant periods of the IG waves and the surging periods of the vessels. On the other hand, relatively small vessels are not affected because their natural (eigen) periods are too short.<sup>82</sup> The reconstruction of harbors and the creation of new harbor elements, can significantly change the harbor resonant periods, either enhancing or, conversely, reducing the surging.<sup>f</sup> Another important aspect of the problem is that ship and mooring lines create an entirely separate oscillation system.<sup>79</sup> Changing the material and the length of the lines and their position,

<sup>f</sup>A famous example of this kind is the French port Le Havre. Before World War II it was known for very common and strong surging motions that created severe problems for ships. During the war a German submarine torpedoed by mistake a rip-rap breakwater, creating a second harbor opening of 20–25 m width. After this, the surging in the port disappeared.<sup>68</sup>

changes the resonant properties of the system (analogous to changing the material and the length of a pendulum).

It is important to keep in mind that each oscillation mode has a specific spatial distribution of sea level variability and associated current (as emphasized in Sec. 9.2.1, maximum currents are observed near the nodal lines). The intensity of the currents varies significantly from place to place. Moreover, topographic irregularities within the harbor and the presence of structure elements (dams, dykes, piers and breakwaters) can create intense local vortexes that may significantly affect the ships.<sup>67</sup> So, the effect of surging on a ship strongly depends on the exact location of the ship, and even on its orientation, in the harbor.

In summary, harbor oscillations arise through co-oscillation of sea surface elevations and currents in the harbor with those at the entrance to the harbor. Seiche-generating motions outside the harbor typically have periods of several minutes and most commonly arise from *bound* and *free long waves* that are incident on the harbor entrance.

### 9.3.3. *Tsunami*

Tsunami waves are the main factor creating destructive seiche oscillations in bays, inlets and harbors.<sup>30,41,53,54,95</sup> Tsunamis can produce “energies” of  $10^3\text{--}10^5\text{ cm}^2$ , although such events are relatively rare (depending on the region, from once every 1–2 years to once every 100–200 years). The main generation mechanisms for tsunamis are major underwater earthquakes, submarine landslides and volcanic explosions. Great catastrophic trans-oceanic tsunamis were generated by the 1946 Aleutian (magnitude  $M_w = 7.8$ ), 1952 Kamchatka ( $M_w = 9.0$ ), 1960 Chile ( $M_w = 9.5$ ), and 1964 Alaska ( $M_w = 9.2$ ) earthquakes. The events induced strong seiche oscillations in bays, inlets, and harbors throughout the Pacific Ocean.<sup>90</sup>

The magnitude  $M_w = 9.3$  earthquake that occurred offshore of Sumatra in the Indian Ocean on 26 December 2004 generated the most destructive tsunami in recorded history. Waves from this event were recorded by tide gauges around the world, including near-source areas of the Indian Ocean (Fig. 9.7), and remote regions of the North Pacific and North Atlantic, revealing the unmatched global reach of the 2004 tsunami.<sup>42,74,86,88</sup> In general, the duration of tsunami “ringing” increased with increasing off-source distance and lasted from 1.5 to 4 days.<sup>74,75</sup> The recorded oscillations were clearly polychromatic, with different periods for different sites, but with clear dominance of 40–50 min waves at most sites. The analysis of various geophysical data from this event indicates that the initial tsunami source had a broad frequency spectrum, but with most of the energy within the 40–50 min band. Therefore, although tsunami waves at different sites induced local eigen modes with a variety of periods, the most intense oscillations were observed at sites having fundamental periods close to 40–50 min.

Differences in spectral peaks among the various tide gauge records are indicative of the influence of local topography. For example, for the Pacific coast of Vancouver Island (British Columbia), the most prominent peaks in the tsunami spectra were observed for Winter Harbor (period  $\sim 30\text{--}46$  min) and Tofino ( $\sim 50$  min). In fact, the frequencies of most peaks in the tsunami spectra invariably coincide with

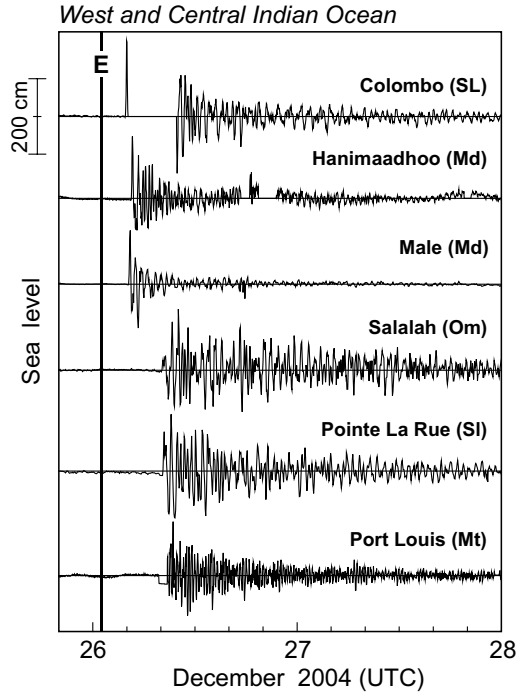


Fig. 9.7. Tsunami records in the Indian Ocean for the 2004 Sumatra tsunami for six selected sites: Colombo (Sri Lanka); Male and Gan (both Maldives); Salalah (Oman); Pointe La Rue (Seychelles); and Port Louis (Mauritius). Solid vertical line labeled “E” denotes the time of the main earthquake shock (from Ref. 74).

corresponding peak frequencies in the background spectra. This result is in good agreement with the well-known fact that periods of observed tsunami waves are mainly related to the resonant properties of the local/regional topography rather than to the characteristics of the source, and are almost the same as those of ordinary (background) long waves for the same sites. For this reason, the spectra of tsunamis from different earthquakes are usually similar at the same location.<sup>30,48,69,g</sup> It is therefore difficult to reconstruct the source region spectral characteristics based on data from coastal stations.

Rabinovich<sup>69</sup> suggested a method for separating the effects of the local topography and the source on the resulting tsunami wave spectrum. This method can be used to reconstruct the open-ocean spectral characteristics of tsunami waves. The approach is based on the assumption that the spectrum  $S(\omega)$  of both the tsunami and background sea level oscillations near the coast can be represented as

$$S(\omega) = W(\omega)E(\omega), \quad (9.24)$$

<sup>g</sup>The resonant characteristics of each location are always the same; however, different sources induce different resonant mode, specifically, large seismic sources generate low-frequency modes and small seismic sources generate high-frequency modes.

where  $W(\omega) = H^2(\omega)$ ,  $H(\omega)$  is the frequency admittance function describing the linear topographic transformation of long waves approaching the coast, and  $E(\omega)$  is the source spectrum. It is assumed that the site-specific properties of the observed spectrum  $S_j(\omega)$  at the  $j$ th site are related to the topographic function  $H_j(\omega)$  for that site, while all mutual properties of the spectra at all sites are associated with the source (assuming that the source is the same for all stations). For typical background oscillations the source spectrum has the form,  $E(\omega) = S_0(\omega)$ , where  $S_0(\omega) = A\omega^{-2}$ , and  $A = 10^{-3} - 10^{-4} \text{ cm}^2$ .<sup>68,69</sup> During tsunami events, sea level oscillations observed near the coast can be represented as

$$\zeta_{\text{obs}}(t) = \zeta_{\text{t}}(t) + \zeta_{\text{b}}(t), \quad (9.25)$$

where  $\zeta_{\text{t}}$  are the tsunami waves generated by an underwater seismic source and  $\zeta_{\text{b}}$  are the background surface oscillations. If the spectra of both tsunami,  $S_{\text{t}}(\omega)$ , and background oscillations,  $\hat{S}_{\text{b}}(\omega)$  and  $S_{\text{b}}(\omega)$  (during and before the tsunami event, respectively) have the form (9.24), and the admittance function,  $W(\omega)$ , is the same for the observed tsunami and the background long waves, then the spectral ratio  $R(\omega)$ , is estimated as

$$R(\omega) = \frac{S_{\text{t}}(\omega) + \hat{S}_{\text{b}}(\omega)}{S_{\text{b}}(\omega)} = \frac{[E(\omega) + \hat{S}_0(\omega)]}{S_0(\omega)} = A^{-1}\omega^2 E(\omega) + 1.0. \quad (9.26)$$

The function  $R(\omega)$ , which is independent of local topographic influence, is determined solely by the external forcing (i.e., by tsunami waves in the open ocean near the source area) and gives the amplification of the longwave spectrum during the tsunami event relative to the background conditions. The close similarity of  $R_j(\omega)$  for various sites confirms the validity of this approach.<sup>69</sup>

The topographic admittance function  $H_j(\omega)$ , which is characteristic of the resonant properties of individual sites, can be estimated as

$$H_j(\omega) = \left[ \frac{S_j(\omega)}{E(\omega)} \right]^{1/2} = \left[ \frac{S_{\text{b}}^j(\omega)}{S_0(\omega)} \right]^{1/2} = \omega \left[ \frac{S_{\text{b}}^j(\omega)}{A} \right]^{1/2}. \quad (9.27)$$

The same characteristic can be also estimated numerically.

### 9.3.4. Seismic waves

There is evidence that seismic surface ground waves can generate seiches in both closed and semi-closed basins. In particular, the Great 1755 Lisbon earthquake triggered remarkable seiches in a number of Scottish lochs, and in rivers and ponds throughout England, western Europe and Scandinavia.<sup>95</sup> Similarly, the Alaska earthquake of 27 March 1964 ( $M_w = 9.2$ ) induced seismic surface waves that took only 14 min to travel from Prince Williams Sound, Alaska, to the Gulf Coast region of Louisiana and Texas where they triggered innumerable seiches in lakes, rivers, bays, harbors, and bayous.<sup>15,34</sup> Recently, the 3 November 2002 Denali earthquake ( $M_w = 7.9$ ) in Alaska generated pronounced seiches in British Columbia and Washington State.<sup>2</sup> Sloshing oscillations were also observed in swimming pools during

these events.<sup>2,15,40</sup> The mechanism for seiche generation by seismic waves from distant earthquakes is not clear, especially considering that seismic waves normally have much higher frequencies than seiches in natural basins. McGarr<sup>40</sup> concludes that there are two major factors promoting efficient conversion of the energy from distant large-magnitude earthquakes into seiches:

- (1) A very thick layer of soft sediments that amplify the horizontal seismic ground motions.
- (2) Deeper depths of natural basins, increasing the frequencies of eigen periods for the respective water oscillations.

It should be noted, however, that seismic origins for seiches must be considered as very rare in comparison, for example, with seiches generated by meteorological disturbances.<sup>95</sup>

### 9.3.5. *Internal ocean waves*

In some regions of the World Ocean, definitive correlation has been found between tidal periodicity and the strong seiches observed in these regions. For example, at Palawan Island in the Philippines, periods of maximum seiche activity are associated with periods of high tides.<sup>21</sup> Bursts of 75-min seiches in the harbor of Puerto Princesa (Palawan Island) are assumed to be excited by the arrival at the harbor entrance of internal wave trains produced by strong tidal current flow across a shallow sill located about 450 km from the harbor.<sup>8</sup> Internal waves can have quite large amplitudes; furthermore, they can travel over long distances without noticeable loss of energy. Internal waves require 2.5 days to travel from their source area in the Sulu Sea to the harbor of Puerto Princessa, resulting in a modulation of the seiche oscillations that are similar to those of the original tidal oscillations.

Similarly, large amplitude seiches on the Caribbean coast of Puerto Rico are also related to tidal activity and are usually observed approximately seven days after a new or full moon (syzygy). Highest seiches in this region occur in late summer and early fall, when thermal stratification of the water column is at its annual maximum. The seven-day interval between syzygy and maximum seiche activity could be accounted for in terms of internal tidal soliton formation near the southwestern margin of the Caribbean Sea.<sup>34</sup> A theoretical model of seiche generation by internal waves, devised by David Chapman (Woods Hole Oceanographic Institution), demonstrated that both periodic and solitary internal waves can generate coastal seiches.<sup>8,20</sup> Thus, this mechanism can be responsible for the formation of seiches in highly stratified regions.

### 9.3.6. *Jet-like currents*

Harbor oscillations (coastal seiches) can also be produced by strong barotropic tidal and other currents. Such oscillations are observed in Naruto Strait, a narrow channel between the Shikoku and Awaji islands (Japan), connecting the Pacific Ocean and

the Inland Sea. Here, the semi-diurnal tidal currents move large volumes of water back and forth between the Pacific and the Inland Sea twice per day with typical speed of 13–15 km/h. This region is one of the greatest attractions in Japan because of the famous “Naruto whirlpool”, occurring twice a month during spring tides, when the speed of tidal flow reaches 20 km/h. Honda et al.<sup>30</sup> noticed that flood tidal currents generate near both coasts significant seiche oscillations with a period of 2.5 min, which begin soon after low tide and cease near high tide; the entire picture repeats with a new tidal cycle. No seiches are observed during ebb tidal currents (i.e., between high and low water) when the water is moving in the opposite direction.

Nakano<sup>57</sup> explained this phenomenon by assuming that a strong current passing the mouth of a bay could be the source of bay seiches, similar to the way that a jet of air passing the mouth piece of an organ pipe produces a standing oscillation within the air column in the pipe. Special laboratory experiments by Nakano and Abe<sup>58</sup> demonstrated that jet-like flow with a speed exceeding a specific critical number generates a chain of antisymmetric, counter-rotating von Karman vortices on both sides of the channel. The checker-board pattern of vortices induce standing oscillations in nearby bays and harbors if their fundamental periods match the typical vortex periods,

$$T_{\text{vor}} = \frac{l}{u}, \quad (9.28)$$

where  $l$  is the distance between vortices, and  $u$  is the speed of the vortices ( $u = 0.4V$  to  $0.6V$ , where  $V$  is the speed of the tidal currents). For the parameters of the Naruto tidal currents, the laboratory study revealed that values of  $T_{\text{vor}}$  agreed with the observed seiche period of 2.5 min. Apparently, the same mechanism of seiche generation can also work in other regions of strong jet currents.

### 9.3.7. Ice cover and seiches

It seems clear that ice cannot generate seiches (except for the case of calving icebergs or avalanches that generate tsunami-like waves). However, an ice cover can significantly impact seiche motions, suppressing them and impeding their generation. At the same time, strong seiches can effectively break the ice cover and promote polynya creation.

Little is known on the specific aspects of ice cover interaction with seiche modes. Hamblin<sup>26</sup> suggested that the ice cover in Lake Winnipeg influences the character of seiche activity. Schwab and Rao<sup>83</sup> assumed that absence of certain peaks in the sea level spectra for Saginaw Bay (Lake Huron) in winter may have been due to the presence of ice cover. Murty<sup>55</sup> examined the possible effect of ice cover on seiche oscillations in Kugmallit Bay and Tuktoyaktuk Harbor (Beaufort Sea) and found that the ice cover reduces the effective water depth in the bay and harbor and in this way diminishes the frequency of the fundamental mode: in Kugmallit Bay from 0.12 cph (ice-free period) to 0.087 cph (ice-covered); and in Tuktoyaktuk Harbor from 1.0 cph to 0.9 cph.

#### 9.4. Meteorological Tsunamis

As discussed in Sec. 9.3.3, tsunamis are the main source of destructive seiches observed in various regions of the World Ocean. However, atmospheric disturbances (atmospheric gravity waves, pressure jumps, frontal passages, squalls) can also be responsible for significant, even devastating, long waves, which have the same temporal and spatial scales as typical tsunami waves. These waves are similar to ordinary tsunami waves and can affect coasts in a similar damaging way, although the catastrophic effects are normally observed only in specific bays and inlets. Nomitsu,<sup>61</sup> Defant,<sup>10</sup> and Rabinovich and Monserrat<sup>71,72</sup> suggested to use the term “*meteorological tsunamis*” (“*meteotsunami*”) for this type of waves.

At certain places in the World Ocean, these hazardous atmospherically induced waves occur regularly and have specific local names: “*rissaga*” in the Balearic Islands, “*šćiga*” on the Croatian coast of the Adriatic Sea, “*marubbio*” (“*marrobio*”) in Sicily, “*milghuba*” in Malta, “*abiki*” and “*yota*” in Japan, “*Seebär*” in the Baltic Sea, “*death waves*” in Western Ireland, “*inchas*” and “*lavadiads*” in the Azores and Madeira islands. These waves are also documented in the Yellow and Aegean seas; the Great Lakes; northwestern Atlantic; Argentina and New Zealand coastal areas; and Port Rotterdam.<sup>7,9–12,16,27,29,30,34,43,51,64,68,71,72,91,92</sup> Table 9.5 gives a list of destructive harbor oscillations, which apparently have the same atmospheric origin and similar resonances due to similarities in the characteristics of the atmospheric disturbances and local geometry and topography of the corresponding basins. Because of the strong likeness between “*meteotsunamis*” and seismically generated tsunamis,<sup>51,88</sup> it is quite difficult sometimes to recognize one from another. Catalogues of tsunamis normally contain references to numerous “*tsunami-like*” events of “*unknown origin*” that are, in fact, atmospherically generated ocean waves.

“*Rissaga*” (a local Catalan word that means “*drying*”, similar to a Spanish word “*resaca*”) is probably the best known example of meteorological tsunamis.<sup>h</sup> These significant short-period sea level oscillations regularly occur in many bays and harbors of the Catalan and Valencian coasts of the Iberian Peninsula, and on the coast of the Balearic Islands. The waves in Ciutadella Harbor, Menorca Island [Fig. 9.8(a)] are particularly high and occur more frequently than in any other location.<sup>18,22,49–51,71–73,81,85</sup>

Ciutadella Inlet is about 1 km long, 100 m wide, and 5 m deep; the harbor is located at the head of the inlet [Fig. 9.8(a)]. The fundamental period of the inlet (Helmholtz mode) is approximately 10.5 min [Figs. 9.8(b,c)]. Due to the particular geometry of Ciutadella Inlet, it has a large  $Q$ -factor, which results in significant resonant amplification of long-wave oscillations arriving from the open sea. Seiche

---

<sup>h</sup>For this reason Derek Goring, a wave specialist from New Zealand, suggested to apply the term “*rissaga*” to all *rissaga*-like meteorological seiches in other areas of the World Ocean.<sup>23</sup> However, if we were to adopt this term, then we would lose information on the cause of the oscillations and the fact that they are part of a family of events that include seismically generated tsunamis, landslide tsunamis, volcanic tsunamis, and *meteotsunamis*.

Table 9.5. Extreme coastal seiches in various regions of the World Ocean.

Region	Local name	Typical period	Maximum observed height	References
Nagasaki Bay, Japan	Abiki	35 min	4.78 m	Honda <i>et al.</i> <sup>30</sup> Amano [1957], Akamatsu <sup>1</sup> , Hibiya and Kajiura <sup>29</sup>
Pohang Harbor, Korea	—	25 min	>0.8 m	Chu [1976], Park <i>et al.</i> [1986]
Longkou Harbor, China	—	2 h	2.93 m	Wang <i>et al.</i> <sup>93</sup>
Ciudadella Harbor, Menorca I., Spain	Rissaga	10.5 min	>4.0 m	Fontseré, <sup>17</sup> Tintoré <i>et al.</i> , <sup>88</sup> Monserrat <i>et al.</i> , <sup>49–51</sup> Gomis <i>et al.</i> , <sup>22</sup> Garcies <i>et al.</i> , <sup>18</sup> Rabinovich and Monserrat, <sup>71,72</sup> Rabinovich <i>et al.</i> <sup>73</sup>
Gulf of Trieste, Italy	—	3.2 h	1.6 m	Caloi [1938], Greco <i>et al.</i> [1957], Defant, <sup>10</sup> Wilson <sup>95</sup>
West Sicily, Italy	Marrubio (Marrobbio)	~15 min	>1.5 m	Plattania [1907], Oddone [1908], Defant, <sup>10</sup> Colucci and Michelato, <sup>9</sup> Candela <i>et al.</i> <sup>7</sup>
Malta, Mediterranean	Milghuba	~20 min	~1.0 m	Airy [1878], Drago <sup>16</sup>
West Baltic, Finland coast	Seebär	—	~2.0 m	Doss [1907], Meissner [1924], Defant, <sup>10</sup> Credner [1988],
Croatian coast	Šćiga	10–30 min	~6.0 m	Hodžić [1979/1980]; Orlić <sup>60</sup> ;
East Adriatic	—	10–40 min	2.0–3.0 m	Vilibić <i>et al.</i> <sup>92</sup> ; Monserrat <i>et al.</i> <sup>51</sup>
Newfoundland, Canada	—	10–40 min	2.0–3.0 m	Mercer <i>et al.</i> [2002]
Western Ireland	Death Waves	?	?	Berninghausen [1964], Korgen <sup>34</sup>
Azores Is and Madeira Is, East Atlantic	Inchas, Lavadiads	?	?	Berninghausen [1964], Korgen <sup>34</sup>
Rotterdam Harbor, The Netherlands	—	85–100 min	>1.5 m	de Loeff and Veldman [1994], de Jong <i>et al.</i> , <sup>11</sup> de Jong and Battjes <sup>12</sup> [2005]

Comment: Exact references can be found in: Wiegel (1964), Korgen (1995), Rabinovich and Monserrat (1996), de Jong *et al.* (2003) and Monserrat *et al.* (2006).

oscillations of duration ranging from a few hours to several days and wave heights exceeding 0.5 m recur in Ciudadella every summer. However, rissaga events (large-amplitude seiches) having wave heights more than 3–4 m, with dramatic consequences for the harbor, usually take place once in 5–6 years. During the rissaga of 21 June 1984 (Fig. 9.9), about 300 boats were destroyed or strongly damaged.<sup>71</sup> More recently, on 15 June 2006, Ciudadella Harbor was affected by the most dramatic rissaga event of the last 20 years, when almost 6-m waves were observed in the harbor and the total economic loss was of several tens millions of euros.<sup>51</sup>

Fontseré,<sup>17</sup> in the first scientific paper on extreme seiches for the Catalan coast, showed that these seiches always occur from June to September and first suggested their atmospheric origin. This origin of rissaga waves was supported by



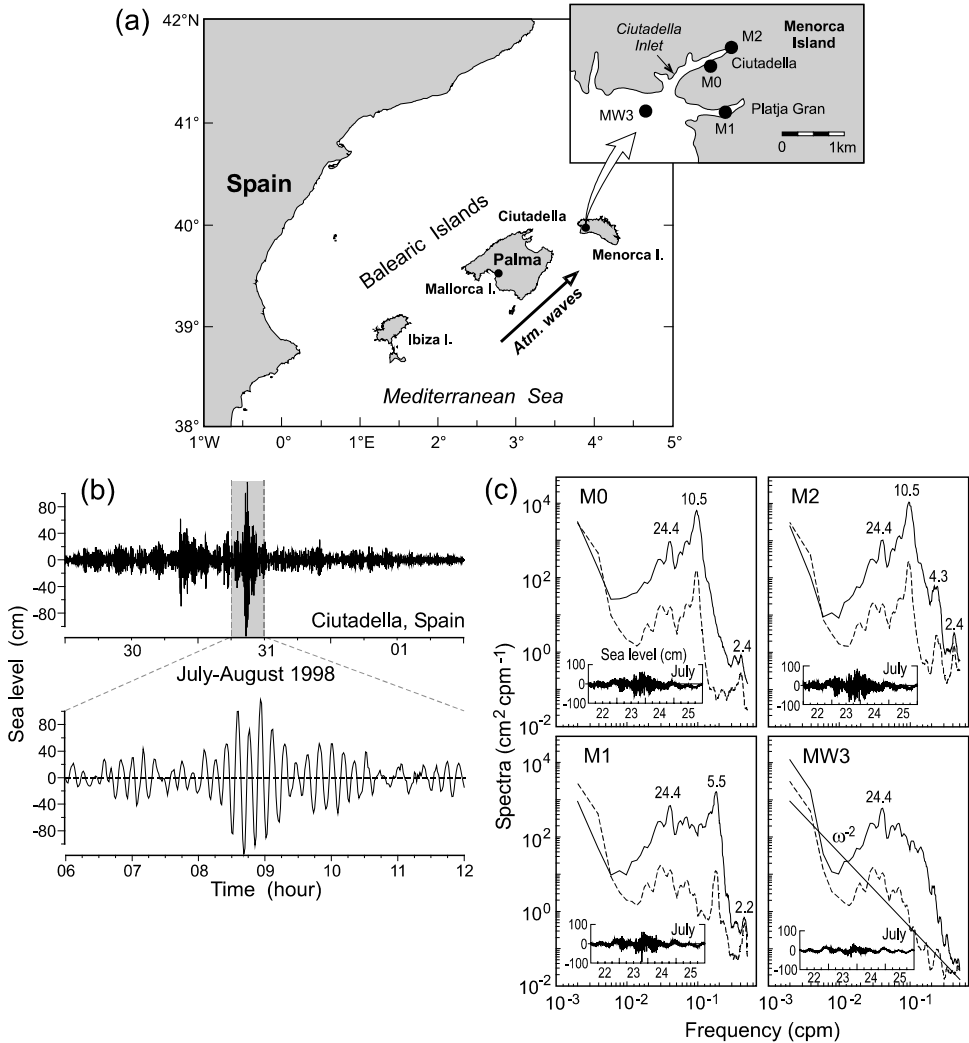


Fig. 9.8. A map of the Balearic Islands and positions of four tide gauges (M0, M1, M2 and MW3) deployed in Ciutadella and Platja Gran inlets and on the shelf of Menorca Island during the LAST-97 experiment.<sup>50</sup> The arrow shows the predominant direction of propagation of atmospheric waves during "rissaga" events. (b) The strong "rissaga" event recorded in Ciutadella Inlet on 31 July 1998 by a tide gauge located at position M0. (c) Spectra for "rissaga" of 24 July 1997 (solid line) and background oscillations (dashed line) for four tide gauges indicated in (a). The actual four-day records during this event are shown in the insets.

Ramis and Jansà<sup>81</sup> based on observed oscillations on the Balearic Islands. These authors also defined a number of typical synoptic atmospheric conditions normally associated with rissaga events. The atmospheric source of *rissaga* is now well established.<sup>18,22,49,50,85</sup> During late spring and summer, meteorological conditions in



Fig. 9.9. Ciutadella Harbor during the rissaga of 21 June 1984. Photo by Josep Gornes (from Ref. 71).

the western Mediterranean are favorable for the formation of high-frequency atmospheric pressure disturbances with parameters promoting the generation of rissaga waves. These conditions include the entrance of warm air from the Sahara at near-surface levels, and relatively strong middle level winds from the southwest. When this synoptic meteorological situation exists, trains of atmospheric pressure gravity waves (with periods of minutes) are reported traveling from SW to NE.<sup>49</sup> If these atmospheric pressure disturbances propagate from SW to NE with a phase speed of about 22–30 m/s, resonant conditions are set up for the southeastern shelf of Mallorca Island (“*Proudman resonance*”) and dynamic energy associated with the atmospheric waves is efficiently transferred into the ocean waves. When these waves reach the coast of Menorca Island, they can generate significant (and sometimes even hazardous) seiche oscillations inside Ciutadella and other inlets due to harbor resonance.

The  $Q$ -factor for the fundamental Helmholtz mode in Ciutadella Inlet (10.5 min), roughly estimated by Eq. (9.20), is about 9. Spectral estimates based on Eq. (9.23) give a similar value,  $Q \approx 10$ .<sup>73</sup> As shown in Fig. 9.8(b), rissaga oscillations in Ciutadella Inlet have a very regular monochromatic character. Maximum wave heights occur during the fourth to the sixth oscillations, in good agreement with the criterion by Miles and Munk<sup>47</sup> that time of the order of  $Q/\pi$  cycles is necessary for

the harbor oscillations to adjust themselves to external forcing. The peak period of 10.5 min for the Helmholtz mode strongly dominates the spectra for the M0 and M2 gauges located in Ciutadella Inlet [Fig. 9.8(c)] both for rissaga and background spectra, while in the adjacent inlet Platja Gran (M1), where rissaga waves are also observed but weaker than in Ciutadella, the dominant peak associated with the Helmholtz mode is 5.5 min. In contrast, on the shelf (MW3) both peaks are absent and oscillations are significantly weaker.

Spectral analysis results [Fig. 9.8(c)] reveal that harbor resonance is a crucial factor in the formation of rissaga waves, as well as “meteorological tsunamis” in other bays, inlets, and harbors of the World Ocean. Barometric data from the Balearic Islands<sup>49–51,81</sup> as well as from Japan,<sup>29</sup> and Eastern Adriatic Sea<sup>64,91,92</sup> demonstrate that generation of these destructive waves is associated with strong atmospheric disturbances, e.g., trains of atmospheric gravity waves, or isolated pressure jumps. These atmospheric disturbances may have different origin: dynamic instability, orographic influence, frontal passages, gales, squalls, storms, tornados, etc.<sup>24</sup> However, even during the strongest events, the atmospheric pressure oscillations at the meteotsunami scales (from a few minutes to a few hours) reach only 2–6 hPa, corresponding to only a 2–6 cm change in sea level. Consequently, these atmospheric fluctuations may produce significant sea level response only when resonance occurs between the ocean and the atmosphere. During the resonance process, the atmospheric disturbance propagating above the ocean surface generates significant long ocean waves by continuously pumping additional energy into these waves.

Possible resonances that are responsible for the formation of meteorological tsunamis are<sup>68</sup>:

- *Proudman resonance*,<sup>65</sup> when  $U = c$ , i.e., the atmospheric disturbance speed ( $U$ ) equals to the long-wave speed of ocean waves  $c = \sqrt{gh}$ ;
- “*Greenspan resonance*”,<sup>25</sup> when  $U_l = c_j$ , the alongshore component ( $U_l$ ) of the atmospheric disturbance velocity equals the phase speed of the  $j$ th mode of edge waves ( $c_j$ );
- “*shelf resonance*,” when the atmospheric disturbance and associated atmospherically generated ocean wave have a period/wavelength equal to the resonant period/length of the shelf.

These resonant effects may significantly amplify ocean waves approaching the coast. Nevertheless, even strong resonant amplification of atmospherically generated ocean waves normally cannot produce waves with sufficient energy to extensively affect the open coast (for example, a 3–4 hPa pressure jump and a factor of 10 resonant amplification, will only produce ocean wave heights of 30–40 cm). It is when energetic ocean waves arrive at the entrance of a semi-closed coastal basin (bay, inlet, fjord or harbor) that they can induce hazardous oscillations in the basin due to harbor resonance.

On the other hand, intense oscillations inside a harbor (bay or inlet) can only be formed if the external forcing (i.e., the waves arriving from the open sea) are energetic enough. Seismically generated tsunami waves in the open ocean can

be sufficiently energetic even in the absence of additional resonant effects (thus, according to satellite altimetry measurements, tsunami waves generated by the 2004 Sumatra earthquake in the open Indian Ocean had trough-to-crest wave heights of approximately 1.0–1.2 m,<sup>86</sup> while atmospherically generated tsunami-like can reach such potentially dangerous levels only in the case of some external resonance. This is an important difference between tsunami waves and meteotsunamis.

It follows from expression (9.17) that a large  $Q$ -factor is critical but that anomalously pronounced harbor oscillations can only be produced when there is resonant matching between the dominant frequency ( $f$ ) of the arriving (external) waves and an eigen frequency  $f_0$  of the harbor (normally, the eigen frequency of the fundamental — Helmholtz — harbor mode). This means that catastrophic harbor oscillations are the result of a *double resonance effect*<sup>51,68</sup>: (a) *external resonance* between the moving atmospheric disturbances and open-ocean waves; and (b) *internal resonance* between the arriving open-ocean waves and the fundamental eigen mode of the harbor (bay, inlet). An additional favorable factor is the specific direction of the propagating atmospheric waves (and corresponding open-ocean waves) toward the entrance of the harbor (bay).

Summarizing what has been presented above, we can formulate the particular conditions promoting creation of extreme atmospherically induced oscillations near the coast (meteotsunamis) as follows:

- *A harbor* (bay, inlet or fjord) with definite resonant properties and high  $Q$ -factor.
- *The occurrence of strong small-scale atmospheric disturbance* (a pressure jump or a train of internal atmospheric waves).
- *A propagation direction* that is head-on toward the entrance of the harbor.
- *The occurrence of an external resonance* (Proudman, Greenspan or shelf) between the atmospheric disturbance and ocean waves.
- *The occurrence of internal resonance* between the dominant frequency of the incoming open-ocean waves and the fundamental harbor mode frequency.

Due to these necessary levels of matching between the atmospheric disturbance, the open-ocean bathymetry and the shelf-harbor geometries, the direction and speed of the atmospheric disturbance probably are even more important than the actual energy content of the incoming waves. In any case, the necessary coincidence of several factors significantly diminishes the possibility of these events occurring, and is the main reason why this phenomenon is relatively rare and restricted to specific locations.<sup>68</sup>

Honda *et al.*<sup>30</sup> and Nakano and Unoki<sup>59</sup> investigated more than 115 gulfs, bays, inlets, and harbors of the Japanese coast and found that highly destructive seiches (not associated with tsunami waves) occur only in a few of them. Extremely strong seiche oscillations (so-called “*abiki*” waves) are periodically excited in Nagasaki Bay. In particular, the *abiki* waves of 31 March 1979 with periods of about 35 min reached wave heights of 478 cm at the northern end of the bay and killed three people.<sup>1,29</sup>

High meteotsunami risk in certain exceptional locations mainly arises from the combination of shelf topography and coastline geometry coming together to create a multiple resonance effect. The factors (internal and external) of critical importance

are: (1) well-defined resonant characteristics of the harbor (bay, inlet, etc.); and (2) specific properties of the shelf favorable for external resonance (between atmospheric and open-ocean waves) and internal resonance (between arriving open-ocean waves and harbor oscillations). The combination of these factors for some particular sites is like a “time-bomb”: sooner or later it will explode (when the atmospheric disturbance is strong enough and the parameters of disturbance coincide with the resonant parameters of the corresponding topography/geometry). Locations with known regular extreme seiches are just the places for these “time-bombs”.<sup>51</sup>

The catastrophic *abiki* wave event of 31 March 1979 best illustrates the physical mechanisms responsible for the generation of meteotsunamis [Fig. 9.10(a)]. Hibiya and Kajiura<sup>29</sup> (HK in the following text) examined this event in detail and constructed an effective numerical model that agrees well with observational data. Nagasaki Bay is a narrow, elongated bay located on the western coast of Kyushu Island, Japan [Fig. 9.10(b)]; the length of the bay is about 6 km, the width is 1 km, and the mean depth is 20 m. The fundamental period of the bay (Helmholtz mode) is 35 min, and this period prevails in seiche oscillations inside the bay (95% of all observed events) and it was specifically this period that was observed on 31 March 1979.<sup>1</sup> HK noticed that almost all known cases of significant *abiki* waves are associated with pressure jumps. In the case of the 1979 event, there was an abrupt pressure jump ( $\Delta P_a$ ) of 2–6 hPa (according to the observations at several sites) that propagated eastward (more precisely, 5.6° north of east) over the East China Sea with an approximate mean speed  $U = 31$  m/s (Fig. 9.5). HK approximated this jump as  $\Delta P_a = 3$  hPa over a linear increase distance  $L_1 = 28$  km and a linear decrease distance  $L_2 = 169$  km. So, the corresponding static inverted barometer response of sea level was  $\Delta \bar{\zeta} \approx -3$  cm [Fig. 9.10(a)]. Moreover, the depth of the East China Sea between mainland China and Kyushu Island is between 50 and 150 m, and the corresponding long-wave speed  $c \approx 22$ –39 m/s. Thus, it was a classical example of Proudman resonance. HK presented a simple expression describing resonant amplification of forced open-ocean long waves as:

$$\Delta \zeta = \frac{\Delta \bar{\zeta} x_f}{L_1 2}, \quad (9.29)$$

where  $x_f = Ut$  is the distance traveled by the pressure jump during time  $t$ . If  $L_1 = 28$  km and  $x_f = 300$  km [from the source area to the Goto Islands — see Fig. 9.10(b)], then  $\Delta \zeta \approx 16$  cm. More precise numerical computation with realistic two-dimensional bathymetry gives the resonant factor  $\varepsilon = \Delta \zeta / \Delta \bar{\zeta} = 4.3$  and  $\Delta \zeta \approx 12.9$  cm in good agreement with observation. Therefore, due to the resonance, the initial disturbance of 3 cm increased in the open sea by four to five times [Fig. 9.10(a)]. It is interesting to note that the resonant amplification is inversely proportional to  $L_1$  [see Eq. (9.29)], so the faster the change in atmospheric pressure (the more abrupt is the pressure jump), the stronger is the amplification of the generated waves (HK).

According to the HK computations, the outer shelf region between the Goto Islands and the mainland of Kyushu (“Goto Nada”) has resonant periods of 64, 36, and 24 min. The second period (36 min) almost coincides with the fundamental period of Nagasaki Bay (35 min). The Goto Nada shelf did not significantly amplify

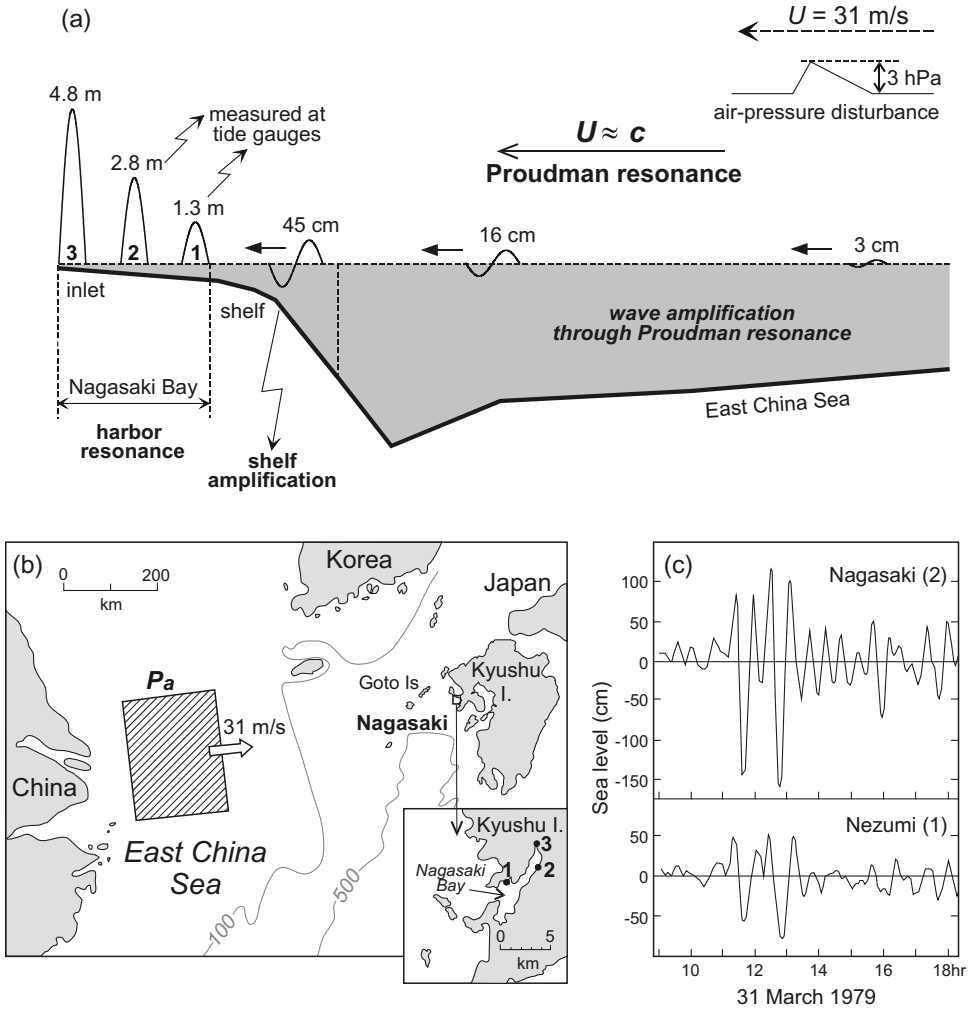


Fig. 9.10. (a) A sketch illustrating the physical mechanism for formation of the catastrophic meteotsunami at Nagasaki Bay (Japan) on 31 March 1979. Numbers “1”, “2”, and “3” correspond to locations shown in (b). (b) Map of Nagasaki Bay and the initial atmospheric pressure disturbance (shaded rectangular region). (c) Tide records of the catastrophic “abiki waves” of 31 March 1979 at Nezumi (9.1) and Nagasaki (2); positions of the tide gauges are shown in the inset in panel (b).

the incoming wave (the first crest height was 16 cm at the shelf depth of 60 m) but it selected and amplified waves with specific periods, in particular those with a period of 36 min. Between the outer sea (depth 60 m) and the head of Nagasaki Bay, the arriving waves were amplified by a factor of 2.4 due to the combined effects of topographic convergence, partial reflection, and shoaling inside the bay. Finally, resonant amplification in Nagasaki of incoming wave train with a period of about 35 min formed catastrophic oscillations within the bay with a maximum recorded

wave height of 278 cm [as measured by a tide gauge located in the middle of the bay — see Fig. 9.10(c)] and an estimated wave height in the head of the bay of 478 cm.<sup>1</sup>

Thus, for this extreme event, we observe the full combination of “hazardous” conditions (factors) responsible for the formation catastrophic oscillations inside Nagasaki Bay: (1) A pronounced atmospheric disturbance (pressure jump of 2–6 hPa), (2) propagating toward the bay with (3) near-resonant phase speed of 31 m/s; this disturbance resonantly generated open-sea long waves with selected (over the shelf) 36 min period that matched (4) the fundamental 35-min period of the bay that has (5) high  $Q$ -factor and well-defined resonant properties. As a result, 3 cm ocean waves in the source area resulted in 478 cm waves at the head of the bay (Fig. 9.4).

Analysis of destructive meteotsunami events in the Mediterranean<sup>18,22,50,51,64,71,72,91,92</sup> indicate that the physical mechanisms of these events were similar to those for Nagasaki Bay event. Tides in the Mediterranean are small; consequently, harbors are not designed to accommodate large amplitude sea level changes associated with occasional meteotsunamis. Consequently, it is atmospherically generated phenomena (not ordinary tsunamis) that are normally responsible for significant flooding and damage in this region. However, the main reason for the damaging nature of meteotsunamis is likely due to the strong currents in the harbor that accompany the sea level oscillations. Seiches with a 10 min period give raise to currents that are 70 times stronger than semi-diurnal tides having the same amplitude.

## Acknowledgments

This work was initiated by Professor Fred Raichlen (CalTech, Pasadena, CA); the author sincerely appreciates his help and friendly support. He is also very grateful to Professor Young Kim (California State University, Los Angeles), the Editor of this Handbook, for his patience and useful comments and to Drs. Sebastian Monserrat (Universitat de les Illes Balears, Palma de Mallorca, Spain) and Ivica Vilibić (Institute of Oceanography and Fisheries, Split, Croatia) for their assistance and providing various observational data. Dr. Richard Thomson (Institute of Ocean Sciences, Sidney, BC, Canada) did tremendous work editing this chapter and encouraging the author, Patricia Kimber (Sidney, BC) helped to draft the figures. Partial financial support was provided by the Russian Foundation on Basic Research, grants 06-0565210a, 08-05-13582, 09-05-00599 and 09-05-01125a and by NATO Science for Peace project SFP-981382.

## References

1. H. Akamatsu, On seiches in Nagasaki Bay, *Pap. Meteor. Geophys.* **33**(2), 95–115 (1982).
2. A. Barberopoulou, A. Qamar, T. L. Pratt and W. P. Steele, Long-period effects of the Denali Earthquake on water bodies in the Puget lowland: Observations and modeling, *Bull. Seism. Soc. Amer.* **96**(2), 519–535 (2006).

3. J. A. Battjes, Surf-zone dynamics, *Ann. Rev. Fluid Mech.* **20**, 257–293 (1988).
4. W. A. M. Botes, K. S. Russel and P. Huizinga, Modeling harbor seiching compared to prototype data, *Proc. 19th Int. Coastal Eng. Conf.*, Houston (1984), pp. 846–857.
5. A. J. Bowen and D. A. Huntley, Waves, long waves and nearshore morphology, *Marine Geol.* **60**, 1–13 (1984).
6. E. C. Bowers, The modelling of waves and their effects in harbors, in *Hydraulic Modelling in Maritime Engineering* (Thomas Telford, London, 1982), pp. 121–127.
7. J. Candela, S. Mazzola, C. Sammari, R. Limeburner, C. J. Lozano, B. Patti and A. Bonnanno, The “Mad Sea” phenomenon in the Strait of Sicily, *J. Phys. Oceanogr.* **29**, 2210–2231 (1999).
8. D. C. Chapman and G. S. Giese, *Seiches, Encyclopedia of Ocean Sciences*, eds J. H. Steele, K. K. Turekian and S. A. Thorpe, Vol. 5 (Academic Press, London, 2001) pp. 2724–2731.
9. P. Colucci and A. Michelato, An approach to study of the ‘Marubbio’ phenomenon, *Boll. Geofis. Theor. Appl.* **13**, 3–10 (1976).
10. A. Defant, *Physical Oceanography*, Vol. 2 (Pergamon Press, Oxford, UK, 1961), 598 pp.
11. M. P. C. de Jong, L. H. Holthuisen and J. A. Battjes, Generation of seiches by cold fronts over the southern North Sea, *J. Geophys. Res.* **108**, 3117 (2003), doi:10.1029/2002JC001422.
12. M. P. C. de Jong and J. A. Battjes, Low-frequency sea waves generated by atmospheric convection cells, *J. Geophys. Res.* **109**, C01011 (2004), doi:10.1029/2003JC001931.
13. V. A. Djumagaliev, E. A. Kulikov and S. L. Soloviev, Analysis of ocean level oscillations in Malokurilsk Bay caused by tsunamis of 16 February 1991, *Science Tsunami Hazards*, **11**, 47–58 (1993).
14. V. A. Djumagaliev, A. B. Rabinovich and I. V. Fine, Theoretical and experimental estimation of transfer peculiarities of the Malokurilsk Bay coast, the Island of Shikotan, *Atmosph. Oceanic Phys.* **30**, 680–686 (1994).
15. W. L. Donn, Alaskan earthquake of 27 March 1964: Remote seiche simulation, *Science* **145**, 261–262 (1964).
16. A. F. Drago, A study on the sea level variations and the ‘Milghuba’ phenomenon in the coastal waters of the Maltese Islands, Ph.D. thesis, University of Southampton (1999).
17. E. Fontseré, Les ‘seixes’ de la costa catalana. Servei Meteorològic de Catalunya, Notes d’Estudi, 58 (1934) (in Catalan).
18. M. Garcies, D. Gomis and S. Monserrat, Pressure-forced seiches of large amplitude in inlets of the Balearic Islands. Part II: Observational study, *J. Geophys. Res.* **101**, 6453–6467 (1996).
19. G. S. Giese and D. C. Chapman, Coastal seiches, *Oceanus* **36**, 38–46 (1993).
20. G. S. Giese, D. C. Chapman, P. G. Black and J. A. Fornshell, Causations of large-amplitude harbor seiches on the Caribbean coast of Puerto Rico, *J. Phys. Oceanogr.* **20**, 1449–1458 (1990).
21. G. S. Giese and R. B. Hollander, The relation between coastal seiches at Palawan Island and tide-generated internal waves in the Sulu Sea, *J. Geophys.* **92**, 5151–5156 (1987).
22. D. Gomis, S. Monserrat and J. Tintoré, Pressure-forced seiches of large amplitude in inlets of the Balearic Islands, *J. Geophys. Res.* **98**, 14437–14445 (1993).
23. D. G. Goring, Rissaga (long-wave events) on New Zealand’s eastern seaboard: A hazard for navigation, *Proc. 17th Australasian Coastal Ocean Eng. Conf.*, 20–23 September 2005, Adelaide, Australia (2005), pp. 137–141.
24. E. E. Gossard and B. H. Hooke, *Waves in Atmosphere* (Elsevier, New York, 1975), 456 pp.



25. H. P. Greenspan, The generation of edge waves by moving pressure disturbances, *J. Fluid Mech.* **1**, 574–592 (1956).
26. P. F. Hamblin, Seiches, circulation and storm surges of an ice-free Lake Winnipeg, *J. Fisheries Res. Board Canada* **33**, 2377–2391 (1976).
27. D. L. Harris, The effect of a moving pressure disturbance on the water level in a lake, *Meteorol. Monogr.* **2**, 46–57 (1957).
28. R. F. Henry and T. S. Murty, Tsunami amplification due to resonance in Alberni Inlet: Normal modes, in *Tsunami: Progress in Prediction, Disaster Prevention and Warning*, eds. Y. Tsuchiya and N. Shuto (Kluwer Acad. Publ., Dordrecht, The Netherlands, 1995), pp. 117–128.
29. T. Hibiya and K. Kajiura, Origin of ‘Abiki’ phenomenon (kind of seiches) in Nagasaki Bay, *J. Oceanogr. Soc. Japan* **38**, 172–182 (1982).
30. K. Honda, T. Terada, Y. Yoshida and D. Isitani, An investigation on the secondary undulations of oceanic tides, *J. College Sci., Imper. Univ. Tokyo* (1908), 108 pp.
31. G. E. Hutchinson, *A Treatise on Limnology. Volume 1. Geography, Physics and Chemistry* (J. Wiley, New York, 1957), 1015 pp.
32. G. H. Keulegan and L. H. Carpenter, Forces on cylinders and plates in an oscillating fluid, *J. Res. Nat. Bureau Stand.* **60**, 423–440 (1958).
33. B. Kinsman, *Wind Waves: Their Generation and Propagation on the Ocean Surface* (Prentice Hall, Englewood Cliffs, 1965), 676 pp.
34. B. J. Korgen, Seiches, *Amer. Sci.* **83**, 330–341 (1995).
35. H. Lamb, *Hydrodynamics*, 6th Edn. (Dover, New York, 1945), 738 pp.
36. J. J. Lee, Wave induced oscillations in harbors of arbitrary geometry, *J. Fluid Mech.* **45**, 375–394 (1971).
37. B. Le Méhauté and B. W. Wilson, Harbor paradox (discussion), *J. Waterways Harbor Division*, ASCE **88**, 173–195 (1962).
38. P. L.-F. Liu, S. Monserrat, M. Marcos and A. B. Rabinovich, Coupling between two inlets: Observation and modeling, *J. Geophys. Res.* **108**, 3069 (2003), doi:10.1029/2002JC001478, 14-(1–10).
39. M. S. Longuet-Higgins and R. W. Stewart, Radiation stress and mass transport in gravity waves, with application to ‘surf-beats’, *J. Fluid Mech.* **13**, 481–504 (1962).
40. A. McGarr, Excitation of seiches in channels by seismic waves, *J. Geophys. Res.* **70**, 847–854 (1965).
41. C. C. Mei, *The Applied Dynamics of Ocean Surface Waves* (World Scientific, London 1992), 740 pp.
42. M. A. Merrifield *et al.*, Tide gage observations of the Indian Ocean tsunami, December 26, 2004, *Geophys. Res. Lett.* **32**, L09603 (2005), doi:10.1029/2005GL022610.
43. M. Metzner, M. Gade, I. Hennings and A. B. Rabinovich, The observation of seiches in the Baltic Sea using a multi data set of water levels, *J. Marine Systems* **24**, 67–84 (2000).
44. G. N. Mikishev and B. I. Rabinovich, *Dynamics of a Solid Body with Cavities Partially Filled with Liquid* (Mashinostroyeniye Press, Moscow, 1968), 532 pp. (in Russian).
45. J. W. Miles, Ring damping of free surface oscillations in a circular tank, *J. Appl. Mech.* **25**, 26–32 (1958).
46. J. W. Miles, Harbor seiching, *Ann. Rev. Fluid Mech.* **6**, 17–36 (1974).
47. J. Miles and W. Munk, Harbor paradox, *J. Waterways Harbor Division*, ASCE **87**, 111–130 (1961).
48. G. R. Miller, Relative spectra of tsunamis, *HIG-72-8 Hawaii Inst. Geophys* (1972), 7 pp.

49. S. Monserrat, A. Ibberson and A. J. Thorpe, Atmospheric gravity waves and the “rissaga” phenomenon, *Q. J. R. Meteorol. Soc.* **117**, 553–570 (1991).
50. S. Monserrat, A. B. Rabinovich and B. Casas, On the reconstruction of the transfer function for atmospherically generated seiches, *Geophys. Res. Lett.* **25**, 2197–2200 (1998).
51. S. Monserrat, I. Vilibić and A. B. Rabinovich, Meteotsunamis: Atmospherically induced destructive ocean waves in the tsunami frequency band, *Nat. Hazards Earth Syst. Sci.* **6**, 1035–1051 (2006).
52. W. H. Munk, Surf beats, *Eos, Trans. Amer. Geophys. Un.* **30**, 849–854 (1949).
53. W. H. Munk, Long waves, *The Sea* (J. Wiley, New York, 1962), pp. 647–663.
54. T. S. Murty, *Seismic Sea Waves — Tsunamis* (Bull. Fish. Res. Board Canada 198, Ottawa, 1977), 337 pp.
55. T. S. Murty, Modification of hydrographic characteristics, tides, and normal modes by ice cover, *Marine Geodesy* **9**, 451–468 (1985).
56. M. Nakano, Secondary undulations in bays forming a coupled system, *Proc. Phys. Math. Soc. Japan* **3**, 372–380 (1932).
57. M. Nakano, Possibility of excitation of secondary undulations in bays by tidal or oceanic currents, *Proc. Imp. Acad. Japan* **9**, 152–155 (1933).
58. M. Nakano and T. Abe, Standing oscillation of bay water induced by currents, *Records Oceanogr. Works in Japan*, Spec. No. 3, 75–96 (1959).
59. M. Nakano and S. Unoki, On the seiches (secondary undulations of tides) along the coast of Japan, *Records Oceanogr. Works Japan*, Spec. No. 6, 169–214 (1962).
60. M. Nakano and N. Fujimoto, Seiches in bays forming a coupled system, *J. Oceanogr. Soc. Japan* **43**, 124–134 (1987).
61. T. Nomitsu, A theory of tsunamis and seiches produced by wind and barometric gradient, *Mem. Coll. Sci. Imp. Univ. Kyoto A* **18**, 201–214 (1935).
62. M. Okihiro, R. T. Guza and R. J. Seymour, Excitation of seiche observed in a small harbor, *J. Geophys. Res.* **98**, 18201–18211 (1993).
63. J. Oltman-Shay and R. T. Guza, Infragravity edge wave observations on two California beaches, *J. Phys. Oceanogr.* **17**, 644–663 (1987).
64. M. Orlić, About a possible occurrence of the Proudman resonance in the Adriatic, *Thalassia Jugoslavica* **16**, 79–88 (1980).
65. J. Proudman, The effects on the sea of changes in atmospheric pressure, *Geophys. Suppl. Mon. Notices R. Astr. Soc.* **2**, 197–209 (1929).
66. D. Prandle, The use of wave resonators for harbor protection, *Dock Harbour Author* (1974), pp. 279–280.
67. A. B. Rabinovich, Possible vorticity effect in longwave motions (surging) in harbors, *Trans. (Doklady) Russian Acad. Sci., Earth Sci. Sec.* **325**, 224–228 (1992).
68. A. B. Rabinovich, *Long Ocean Gravity Waves: Trapping, Resonance, and Leaking* (Gidrometeoizdat, St. Petersburg, 1993), 325 pp. (in Russian).
69. A. B. Rabinovich, Spectral analysis of tsunami waves: Separation of source and topography effects, *J. Geophys. Res.* **102**, 12663–12676 (1997).
70. A. B. Rabinovich and A. S. Levyant, Influence of seiche oscillations on the formation of the long-wave spectrum near the coast of the Southern Kuriles, *Oceanology* **32**, 17–23 (1992).
71. A. B. Rabinovich and S. Monserrat, Meteorological tsunamis near the Balearic and Kuril Islands: Descriptive and statistical analysis, *Nat. Hazards* **13**, 55–90 (1996).
72. A. B. Rabinovich and S. Monserrat, Generation of meteorological tsunamis (large amplitude seiches) near the Balearic and Kuril Islands, *Nat. Hazards* **18**, 27–55 (1998).

73. A. B. Rabinovich, S. Monserrat and I. V. Fine, Numerical modeling of extreme seiche oscillations in the region of the Balearic Islands, *Oceanology* **39**, 16–24 (1999).
74. A. B. Rabinovich, R. E. Thomson and F. E. Stephenson, The Sumatra tsunamis of 26 December 2004 as observed in the North Pacific and North Atlantic oceans, *Surveys Geophys.* **27**, 647–677 (2006).
75. A. B. Rabinovich and R. E. Thomson, The 26 December 2004 Sumatra tsunami: Analysis of tide gauge data from the World Ocean Part 1. Indian Ocean and South Africa, *Pure Appl. Geophys.* **164**, 261–308 (2007).
76. A. B. Rabinovich, L. I. Lobkovsky, I. V. Fine, R. E. Thomson, T. N. Ivelskaya and E. A. Kulikov, Near-source observations and modeling of the Kuril Islands tsunamis of 15 November 2006 and 13 January 2007, *Adv. Geosci.* **14**, 105–116 (2008).
77. B. I. Rabinovich and Y. V. Tyurin, *Numerical Conformal Mapping in Two-Dimensional Hydrodynamics* (Space Research Institute RAS, Moscow, 2000), 312 pp.
78. F. Raichlen, Harbor resonance, *Estuary and Coastline Hydrodynamics*, ed. A. T. Ippen (McGraw Hill Book Co., New York, 1966), pp. 281–340.
79. F. Raichlen, The effect of ship-harbor interactions on port operations, *Maritime Technol.*, 11–20 (2002).
80. F. Raichlen and J. J. Lee, Oscillation of bays, harbors and lakes, *Handbook of Coastal and Ocean Engineering*, ed. J. B. Herbich (Gulf Publishing Company Houston, Texas, 1992), pp. 1073–1113.
81. C. Ramis and A. Jansà, Condiciones meteorológicas simultáneas a la aparición de oscilaciones del nivel del mar de amplitud extraordinaria en el Mediterráneo occidental, *Rev. Geofísica* **39**, 35–42 (1983) (in Spanish).
82. T. Sawaragi and M. Kubo, Long-period motions of a moored ship induced by harbor oscillations, *Coast. Eng. Japan* **25**, 261–275 (1982).
83. D. J. Schwab and D. B. Rao, Gravitational oscillations of Lake Huron, Saginaw Bay, Georgian Bay and the North Channel, *J. Geophys. Res.* **82**, 2105–2116 (1977).
84. R. M. Sorensen and E. F. Thompson, Harbor hydrodynamics, *Coastal Engineering Manual*, Part II (U.S. Army Corps. of Engineers, Washington, D.C., New York, 2002), Chapter 7, pp. 1–92.
85. J. Tintoré, D. Gomis, S. Alonso and D. P. Wang, A theoretical study of large sea level oscillations in the Western Mediterranean, *J. Geophys. Res.* **93**, 10797–10803 (1988).
86. V. V. Titov, A. B. Rabinovich, H. Mofjeld, R. E. Thomson and F. I. González, The global reach of the 26 December 2004 Sumatra tsunami, *Science* **309**, 2045–2048 (2005).
87. R. E. Thomson, P. W. Vachon and G. A. Borstad, Airborne synthetic aperture radar imagery of atmospheric gravity waves, *J. Geophys. Res.* **97**, 14249–14257 (1992).
88. R. E. Thomson, A. B. Rabinovich and M. V. Krassovski, Double jeopardy: Concurrent arrival of the 2004 Sumatra tsunami and storm-generated waves on the Atlantic coast of the United States and Canada, *Geophys. Res. Lett.* **34**, L15607 (2007), doi:10.1029/2007GL030685.
89. M. J. Tucker, Surf beats: Sea waves of 1 to 5 minute period, *Proc. Roy. Soc. London Ser. A* **202**, 565–573 (1950).
90. W. G. Van Dorn, Some tsunami characteristics deducible from tide records, *J. Phys. Oceanogr.* **14**, 353–363 (1984).
91. I. Vilibić and H. Mihanović, A study of resonant oscillations in the Split harbor (Adriatic Sea), *Estuar. Coastal Shelf Sci.* **56**, 861–867 (2003).
92. I. Vilibić, N. Domijan, M. Orlić, N. Leder and M. Pasarić, Resonant coupling of a traveling air-pressure disturbance with the east Adriatic coastal waters, *J. Geophys. Res.* **109**, C10001 (2004), doi:10.1029/2004JC002279.

93. X. Wang, K. Li, Z. Yu and J. Wu, Statistical characteristics of seiches in Longkou harbor, *J. Phys. Oceanogr.* **17**, 1063–1065 (1987).
94. R. L. Wiegel, Tsunamis, storm surges, and harbor oscillations, *Oceanographical Engineering* (Prentice-Hall, Englewood Cliffs, NJ, 1964), Ch. 5, pp. 95–127.
95. B. Wilson, Seiches, *Advances in Hydrosciences* **8**, 1–94 (1972).
96. J.-K. Wu and P. L.-F. Liu, Harbor excitations by incident wave groups, *J. Fluid Mech.* **217**, 595–613 (1990).